EXPLORING THE EFFECTS OF SODIUM BUTYRATE ON CELL MORPHOLOGY, CELL GROWTH, AND EXPRESSION OF A RECOMBINANT ANTI-APOPTOTIC VENUS–BCL-X_L FUSION PROTEIN IN GREEN MICROALGAE *CHLAMYDOMONAS REINHARDTII*

By

Victor Oh

A thesis submitted to the Johns Hopkins University in conformity with the requirements for the degree of Master of Science in Engineering

Baltimore, Maryland
December 2013

BLANK PAGE

ABSTRACT

Green eukaryotic microalgae are an attractive economic, and efficient, alternative to conventional recombinant protein expression systems and have the potential to revolutionize the biotechnology industry. Recent advancements in the genomic and proteomic techniques of microalgae have ushered tremendous efforts to optimize the "upstream" side of process design through the use of promoters, codon-optimization, and plasmid design. While the prospective for microalgae as a molecular farming platform is high, there are still a number of major obstacles, namely inconsistent transgene expression, that must be overcome before it can be implemented as a standard expression system.

The supplementation of culture medium with sodium butyrate to enhance transgene expression in mammalian cells for higher protein yields has been studied for several decades. Despite the wealth of literature available on the role of sodium butyrate in inducing changes of the morphology, growth rate, and gene expression in mammalian and plant cells, there is little information documented on its effect on green microalgal cells. In this study we explore the changes in cell morphology, cell growth, and transgene expression of a recombinant anti-apoptotic Venus-Bcl-x_L protein in microalgae *Chlamydomonas reinhardtii* (*C. reinhardtii*) cells induced by sodium butyrate supplementation, and investigate the prospective of combining the advantages of a genetically modified anti-apoptotic *C. reinhardtii* strain with the transgene enhancing effects of sodium butyrate.

We observed that concentrations of sodium butyrate above 250 mM were lethal for both the wild-type *C. reinhardtii* wall-deficient (*CW 15+*) UTEX 2337 strain and *C. reinhardtii* wall-deficient Venus-Bcl-x_L (pRelax) strain. Concentrations of 50 mM and 100 mM induced phonotypical changes in the wild-type *C. reinhardtii* cell morphology induced apoptosis and inhibited cell growth. The difference in final cell density for cultures induced with 50 mM and 100 mM sodium butyrate from untreated cells averaged 5.79% and 62.92%, respectively. The anti-apoptotic pRelax *C. reinhardtii* strain showed significant signs of tolerance to apoptosis and cell growth inhibition at 50 mM and 100 mM sodium butyrate as cultures treated with 50 mM and 100 mM sodium butyrate were 75% and 78% less apoptotic than untreated pRelax cells, respectively, and difference in final cell density from untreated pRelax cells were -13.08% and 1.675%, respectively. The transgenic pRelax strain induced with 50 mM and 100 mM sodium butyrate showed substantial reduction in apoptotic behavior compared to untreated pRelax cells, indicating the possibility of up-regulation of the recombinant anti-apoptotic Venus-Bcl-x_L protein caused by sodium butyrate induction.

Advisors

Dr. Michael J. Betenbaugh
Professor, Department of Chemical & Biomolecular Engineering
Johns Hopkins University

Dr. George A. Oyler
President, Synaptic Research LLC

Julian N. Rosenberg
Senior Research Scientist, Synaptic Research LLC

Reader

Dr. Marc D. Donohue
Professor, Department of Chemical & Biomolecular Engineering
Johns Hopkins University

AKNOWLEDGMENTS

I would like to thank Dr. Michael Betenbaugh for his guidance and leadership, both throughout my undergraduate and graduate years. Working in his lab has been one of the most fruitful experiences I have had, and I owe a large part of my personal growth to him. I am also extremely grateful for Julian Rosenberg and his incredible mentorship during my graduate studies. It was a privilege to work alongside an individual of such caliber, and each moment was a chance to learn something new.

I would like to also thank my fellow graduate students in the algae team: Bernardo Guzman and Jonathan Rogers. The dynamics of our interaction were always fruitful and always encouraging. I could not have asked for a better group of peers to work passionately and tirelessly with. I am extremely grateful for the team of undergraduates that helped do a bulk of the grunt work: Christian Salera, Mingoo Kim, Brian Chung, Evan, and Nico. It was a pleasure working the lab with a group of dedicated students whom I could trust. I thank Bojiao Yin and Andrew Chung from the mammalian team, for their constant support and guidance through much of the laboratory procedures that were at first new to me.

Finally, I would like to thank my family and friends who are always my strength and support. I love, and thank God for all of you. I dedicate this thesis to them, and to God who made all of this even possible.

TABLE OF CONTENTS

INTRODUCTION

In the early 80's, the Food and Drug Administration (FDA) approved the clinical usage of recombinant human insulin from bacterium *Escherichia coli* (*E. coli*) for the treatment of diabetes. Since then, nearly 200 recombinant pharmaceuticals have entered the market with the approval for human use by the FDA and/or by the European Medicines Agency (EMEA) [1]. Most of the hosts used to produce these proteins are microbial cells such as bacteria and yeast. The difficulty of obtaining therapeutic human proteins from natural sources makes recombinant DNA technology an important tool for the effective and scalable production of pharmaceutical proteins [1].

The use of recombinant proteins has gained huge momentum in recent years, particularly in the biopharmaceutical industry, as advances in genomic and proteomic techniques enabled the development of more complex molecules and approaches. The number of recombinant protein pharmaceutical drugs is expected to surpass 200 over the next few years, all with potential to treat expanding human disorders such as diabetes, cancer, respiratory, cardiovascular and inflammation-related diseases, as well as rare diseases. The global market for protein pharmaceuticals exceeds $50 billion, with an average annual growth rate of almost 4% [2]. However, the development of any new protein-based drug is difficult with the requirements of such high capital investment and operating cost inherent in the production of these molecules. The costs of manufacturing a recombinant protein may constitute nearly 25% of its global sale figures [3]. The core element affecting the

process cost is the biological host used for the recombinant protein production, which creates great motivation to find cost-effective alternatives to current expression platforms [2].

Current expression systems

Although most of the FDA or EMEA approved recombinant pharmaceuticals are hosted by bacteria and yeast, no standard system exists for the efficient and cost-effective production of proteins on a commercial scale. Currently the inherent advantages of each system dictate its preference depending on the situation. For example, bacteria and yeast considered the most economic expression systems, because of their relatively inexpensive media components and operating costs [4]. They are also versatile due to the combination of a large database of physiological information and accessibility of advanced genetic tools. While the initial capital cost of fermentation and purification equipment is relatively expensive, the fermentation systems are simple and media costs are low.

Despite the economic benefits of using bacteria expression systems, their application is limited due to their inability to perform post-transcriptional and post-translational modifications necessary for production of fully functional eukaryotic proteins [5]. While glycosylation is the most common post-translational modification, there are several others that play a critical role in biological activity, protein folding, tissue targeting, immunogenicity, solubility, and stability [1]. Although high levels of expression are achievable in bacteria, the expressed heterologous proteins tend to accumulate

intracellularly as insoluble inclusion bodies [6]. There are also difficulties downstream, as the presence of bacterial endotoxins and proteases makes purification difficult and can lead to adverse effects in humans [7].

Yeasts are as cost effective and fast as bacteria and cell cultures can reach a high density when grown in bioreactors. Approved protein products from yeast are produced solely in *Saccharomyces cerevisiae* (*S. cerevisiae*) [1]. Yeasts are capable of post-translational modification, and thus usually the expression host when the target protein requires a specific post-translational modification for biological activity [8]. While yeasts can perform glycosylation, the glycosylation process is different from that of higher eukaryotes and usually involves hyperglycosylation, which can lead to immunogenic responses in humans [9]. In both bacterial and yeast systems, overproduction of either eukaryotic or prokaryotic recombinant proteins has been found to trigger metabolic and conformational stress in the host cells [1]. The cells stress response can often lead to changes in protein processing resulting in useless products that failed to reach their native conformation [1]. In addition, bacteria and yeast expression systems fail to efficiently produce properly folded full-length molecules with sizes larger than 60 kDa, resulting in poor yields of more complex proteins [1, 4].

Mammalian cell lines are currently the dominant system for the production of diagnostic and therapeutic proteins because of their capacity for proper protein folding, assembly and post-translational modification [10]. However, while these attributes are necessary for the

expression of fully functioning, complex molecules, such as therapeutic proteins, there are several major disadvantages that render mammalian cells inefficient as a standard recombinant pharmaceutical expression platform. Maintaining mammalian cell lines is difficult due to their inherent sensitivity and instability. In addition to extreme capital expenses, high media and protein purification costs cripple economic feasibility. Unlike bacteria and yeast, mammalian cells grow slowly, further hindering large-scale expression. The main danger of using mammalian cells is the potential of contamination of the isolated protein with disease-causing agents or oncogenic sequences [11]. Most of the therapeutic proteins approved thus far have been expressed in Chinese hamster ovary (CHO) cells, mainly for the robustness of the cells to grown in serum free media, protein-free and chemically defined media [1]. Strictly controlling the media reduces risk of infection and immunogenicity, ultimately increasing the biosafety of the final protein products. Another major advantage of using CHO cells as an expression system is that recombinant protein can be secreted directly into the medium, which reduces the complications and costs of downstream purification [12]. Additional to CHO cells, mouse myeloma (NS0), baby hamster kidney (BHK), human embryonic kidney (HEK-293), human cervical cancer (HeLa) cells, and human-retina-derived (PERC6) cells have proved to be relatively good alternatives [13].

Transgenic plants have the major advantage of scalability. Tobacco, for example, can be planted on thousands of acres. Thus, these plant expression systems can be grown on an agricultural scale. Additionally the production costs are much lower than bacterial, yeast,

and mammalian systems because of the plants' inherent photosynthetic mechanisms. Like yeasts and mammalian bioreactors, plants are able to produce fully functional proteins. This combination of scalability and efficacy give terrestrial plants potential as a powerful platform for recombinant protein expression. However, a major drawback of this system is its low production rate. The time frame between initial transformation and having the appropriate amount of protein (mg to g) can be over two or three years. Additionally, expressing human therapeutics in plants is the threat of gene transfer to surrounding food crops [4]. However, the main disadvantage of using transgenic plants is related once again to post-translational modifications. Plant-specific glycosylation pathways introduced in recombinant proteins produce immunogenic responses in humans [9].

The major prohibitive factors for a standard recombinant protein expression system are the high capital investment and production costs inherent in the current expression platforms. The high prices of protein drugs reflect the costs, which often make them inaccessible to many patients who are in need of the drugs. For example recombinant human Erythropoietin (EPO), used to treat anemia costs over $2 billion/kg. Enzyme replacement therapies such as for lysosomal storage diseases (LSD) represent in excess of $150,000/year per patient [13]. To make these crucial protein therapeutic treatments more widely accessible, a greater cost-effective, yet fully functional, expression system is needed as an economically viable alternative.

Potential of microalgae as a protein expression platform

Eukaryotic microalgae are an attractive alternative to current models in use and have the potential to revolutionize biotechnology. The growth rate of algae is much faster compared to terrestrial plants. For example, microalgae like *Chlamydomonas reinhardtii* (*C. reinhardtii*) double cell number in approximately 8 hours under a 12-hour light, 12-hour dark regime. Time from initial transformation to protein production can be as little as six weeks and scale-up from flasks to a commercially viable scale can be just a few months [4]. Like plants, the algae can be cultivated at low productions costs as they require only water and nutrients, but there is no risk for transgene flow to food crops as the algae can be contained in photo bioreactor cultures. Additionally, microalgae's protein content ranges from 50 – 70% of its fresh weight, which is a much higher percentage than the choicest edible parts of any higher plant or animal [14].

The unicellular green microalgae *C. reinhardtii* is a fantastic model organism for the study of a broad range of biological uncertainties in areas such as flagellar function, photobiology, and photosynthesis research [15, 16, 17, 18]. The nuclear, chloroplast, and mitochondrial genomes have been fully sequenced and can be transformed [19]. It can reproduce sexually or asexually and can grow photoautotrophically, heterotrophically or mixotrophically. The completion of the *Chlamydomonas* genome-sequencing project in 2007, provided new insights into the evolution of photosynthetic eukaryotes, and paved the way for exploitation of the alga as a model system in plant post-genomics research [20, 21].

The chloroplast organelle of plant and eukaryotic microalgal cells, like *C. reinhardtii*, hosts many important biosynthetic pathways, such as photosynthesis, and also serves as a storage compartment [22]. *C. reinhardtii* has one large chloroplast that fills approximately 40% of the cell by volume. The chloroplast genome is a 203 kb circular molecule and encodes for approximately 100 genes [23]. Each chloroplast has about 80 identical copies of each genome. Inherently, the chloroplast is capable of accumulating substantial amounts of membrane proteins (i.e. photosystems I and II) and soluble proteins (i.e. enzymes like RuBisCO) along with other macromolecules such as chlorophylls, carotenoids, starch and lipids. The intrinsic function of the chloroplast makes it an attractive platform from a recombinant-genetics perspective [22].

In a recent study on recombinant antibody production, the cost of production per gram of functional antibody was only US $0.002 in microalgae, while $150 and $0.05 in mammalian and plant expression systems, respectively [24]. Additionally, microalgae contain all the advantages of post-translational and post-transcriptional modifications and are efficient at folding and producing complex, functional proteins. Algae are also generally regarded as safe (GRAS), which make them potentially valuable for oral delivery vehicle of therapeutic proteins with little to no purification.

However, despite its rapid growth and high biomass production at low cost, prospects for microalgae as an efficient production platform for recombinant proteins as

biopharmaceuticals, has been severely hampered by the very low expression levels usually obtained for transgenes in C. *reinhardtii* [21].

CHAPTER ONE: GENETIC ENGINEERING OF MICROALGAE *CHLAMYDOMONAS REINHARDTII*

Although recombinant protein expression at commercially viable levels has only been reported for expression from the chloroplast genome, both the nuclear and mitochondrial genomes have achieved successful recombinant protein expression [25].

BACKGROUND

There are several reasons that the chloroplast may be considered more advantageous than the nucleus in expressing transgenes for recombinant products [26]. Transformation in the chloroplast, in contrast to transformation in the nucleus, is almost exclusively executed through homologous recombination. Thus, the transgene inserted into the plastome can be site-specific leading to precise and predictable manipulation. Nuclear transformation is primarily performed by random insertion through non-homologous end joining, which can lead to many undesirable side effects, because genes coding for regulatory elements can be disrupted [27]. Alternatively, homologous recombination through chloroplast transformation enables precise targeting of "silent sites," or regions void of any known coding sequences [28]. While, the highest reported protein expression level in the chloroplast is slightly over 10% total soluble protein (TSP), the majority of yields average around 5% TSP [29, 30]. In contrast, an expression level of 0.2% TSP achieved from nuclear expression is relatively high [21].

The potential and limitation of genetic engineering the nuclear genome

Despite the low yields of recombinant protein expression from nuclear expression, the possibilities for post-transcriptional, post-translational modifications, and post-translational targeting to specific intracellular organelles make nuclear expression necessary for complex protein expression [25]. While the reasons for low nuclear expression are still poorly understood, positional effects, RNA silencing, a prohibitively compact chromatin structure, and non-conventional epigenetic effects have been anticipated as possible reasons [25].

The impact of promoters

For high recombinant protein yields, the plasmid-construct design should reflect an optimal system from all stages of gene expression, from gene transcription to protein stability. The most important elements for high-level transcription are the promoters and 5'/3' regulatory untranslated regions (UTRs) [31]. In general, functional promoters regulate transcription, 5' UTR mediate mRNA stabilization, and translation initiation, and 3'-UTR mediate stability and act in the termination of transcription [32]. Improvements in recombinant protein expression in algae can be largely credited to advancements in identifying functional promoter sequences. Flanking the transgene of interest with a proper promoter, and its respective 5'/3' UTRs, is important for high-level transcription. These sequences are distinctive depending on different microalgal strains and genes. Even within the cell the promoter sequences are different with respect to cell localization [32].

Codon bias optimization

Along with promoters and 5'/3' UTR sequences, codon dependency is an important limiting factor for the high expression of transgenic protein in microalgae. Different organisms can use certain codons more frequently than others, leading to a contrary bias in codon usage between host cells. This causes shifts in tRNA abundance potentially leading to translational stalling, premature translation termination, translation frame shifting and amino acid misincorporation [33]. An example of such codon dependency can be found in C. *reinhardtii*, which has an extremely high GC content (~61%) [34]. It has also been observed that codons containing adenine or thiamine nucleotides in the third position favored over those with guanine or cytosine [35]. In 2002 Franklin, *et al,* tested the effects of codon dependency in the C. *reinhardtii* chloroplast by developing a gene encoding green fluorescent protein (GFP) *de novo*, which has been codon optimized to the C. *reinhardtii* chloroplast genome. Protein expression levels of codon-optimized GFP was compared to that of a non-optimized GFP, both under the control of an *rbcL* promoter and 5'/3' UTRs. A 80-fold increase in GFP accumulation was observed in the case where C. *reinhardtii* was transformed with codon-optimized GFP [36].

Genetic transformation of cell wall-deficient *C. reinhardtii*

The removal of the cell walls from C. *reinhardtii* wild-type strains significantly increases the number of successful transformants. The mating of mating type plus (mt+) with mating type minus (mt-) gametes of C. *reinhardtii* creates cell wall-deficient strains, by the release of enzymes that cause cell wall degradation during flagellar interaction [37]. There are several

techniques developed for the delivery of DNA to the target microalgal genomes that are still being applied and studied in recent research. Although these transformation methods are done with wall-deficient strains, the efficiencies successful for transformants are still very low [25].

Glass beads method

Transformation by glass beads is a simple and effective technique that involves agitating wall-deficient cells with linearized, recombinant DNA and sterile glass beads. Although the intensity of the agitation affects the viability of the transformed cells, efficiencies of 10^3 transformants/μg DNA for nuclear transformation and 50 transformants/μg DNA for chloroplast transformation were observed [38, 39].

Particle bombardment

The particle bombardment method has been shown to be effective for the stable transformation of the nuclear and chloroplast genomes of *C. reinhardtii* [38, 40]. The technique involves the bombardment of target algae cells with metallic particles, usually gold or tungsten, which are coated in DNA. The transformation efficiency can be especially low due to the fatal effect of the bombard on the cells. However, it remains to be the most effective method for transformation of the chloroplast, because it allows the penetration of the recombinant DNA through both the cell membrane and chloroplast membrane, for successful integration [41]. The method is significantly more expensive, because it requires

specialized equipment, and thus less preferred over glass beads or electroporation methods for nuclear transformation.

Electroporation

Transformation by electroporation is two orders of magnitude higher in transformation efficiency compared to the glass beads method [42]. It exposes the cell walls to high intensity electrical field pulses that induce macromolecular uptake and disrupt lipid bilayers, leading to efficient molecular transport across the plasma membrane [43, 44]. Electroporation only requires relatively simple equipment, compared to particle bombardment, but is dependent on important parameters including field strength, pulse length, medium composition, temperature, and membrane characteristics [42, 43].

Agrobacterium tumefaciens

Another method of delivering recombinant DNA is by transformation with tumor-inducing *Agrobacterium tumefaciens* [25]. While this method has been mainly used for the modification of plant cells, *C. reinhardtii* has been successfully transformed by this method with recorded transformation efficiencies that are fifty times greater than the glass-beads method [45]. Although, transformation of microalgae with *Agrobacterium* is still a field in its infancy, the method has considerable promise, and is currently a widely pursued area of research [25].

MATERIALS & METHODS

pVenus and pRelax plasmid overview:

The two vectors used to transform *C. reinhardtii* wall-deficient strain UTEX 2337 (*CW 15+*) are outlined below (*see Figures 1a and 1b*). Both vectors have been codon-optimized to the nuclear genome.

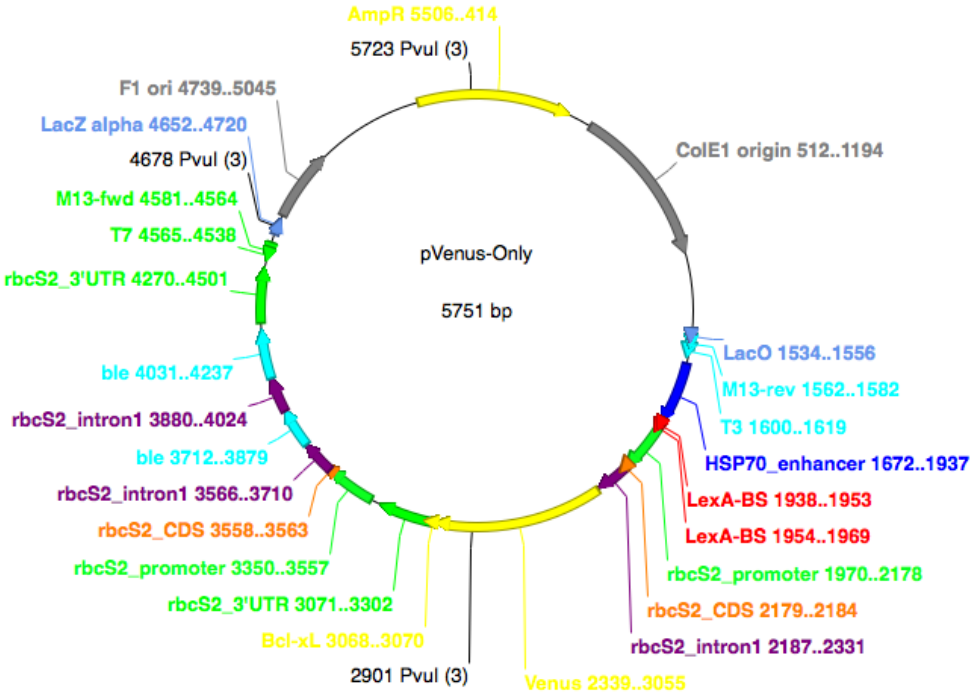

Figure 1a: Vector map of pVenus plasmid with Pvu1 restriction enzyme sites. Expected band lengths (bp): 2929, 1777, 1045.

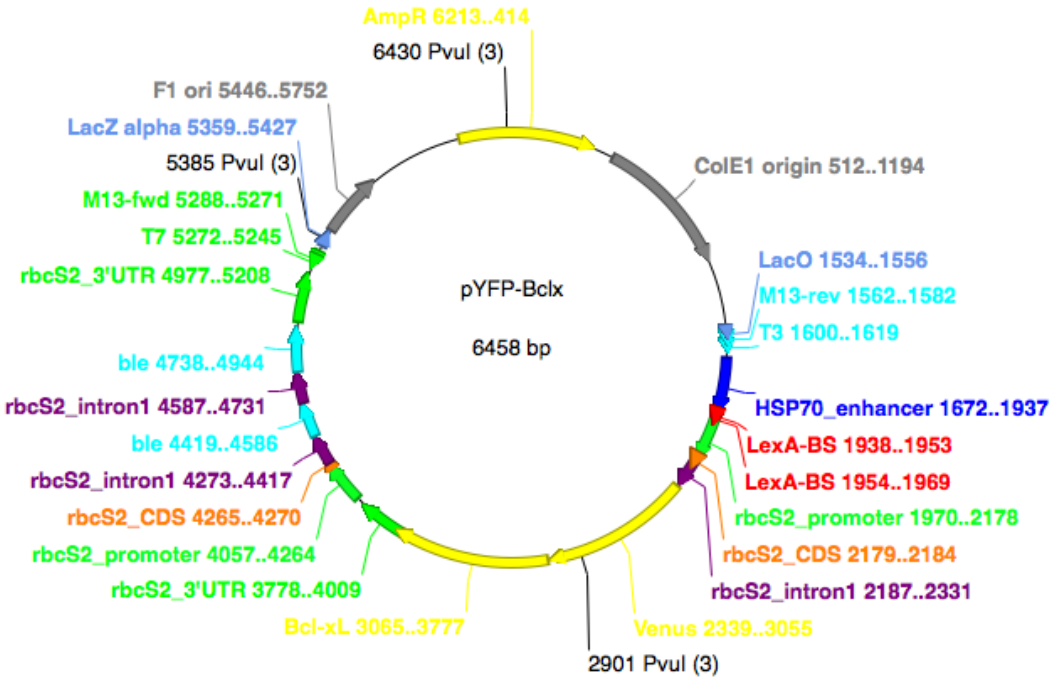

Figure 1b: Vector map of pVenus-Bcl-x_L (pRelax) plasmid with PvuI restriction enzyme sites. Expected band lengths (bp): 2929, 2484, 1045.

Both the pVenus and pRelax vector were designed by *Rosenberg, et al* [46]. The Venus protein is a fluorescent reporter, which has been shown to have higher fluorescence than a similar fluorescent marker yellow fluorescent protein. In the case of the pRelax plasmid, the Venus is immediately upstream of the anti-apoptotic Bcl-x_L gene, which is ultimately translated into a Venus-Bcl-x_L fusion protein [47]. The Bcl-x_L protein has been shown to prevent programmed cell death in a number of mammalian and plant cells [48, 49]. The plasmids are designed to have the *HSP70* (heat shock protein 70) promoter fused upstream of a *RBCS2* (rubisco) promoter, which has been shown to significantly improve driving transgene expression and transformation efficiency in *C. reinhardtii* [50, 51]. Both plasmids also have a bacterial resistance gene *ble*, which is needed for selecting successfully transformed colonies.

pVenus and pRelax Plasmid DNA Purification:

Glycerol stocks of pVenus and pRelax plasmids were received from Synaptic Research LLC in Baltimore, MD. Glycerol stocks were lightly brushed using 200 µL pipet tips, and pipet tips were dispensed into 3 mL of Luria Broth medium (Sigma-Aldrich, St. Louis, MO). 3 mL of bacterial culture, DH5α, were grown overnight for 16 hours. 1 mL of each culture were pipetted and harvested by centrifugation for subsequent DNA plasmid purification. Remaining 2 mL of each bacterial culture were stored at 4 °C to be further scaled up.

DNA plasmids were purified using a QIAprep Spin Miniprep Kit (QIAGEN, USA Cat# 27104). Purified DNA samples for pVenus and pRelax were eluted into 1.5 mL microcentrifuge tubes and stored at -20 °C for further restriction enzyme digest analysis.

Restriction Enzyme Diagnostic Digest of pVenus and pRelax Plasmids

Purified DNA plasmids from mini-prep were analyzed by restriction enzyme digest to confirm presence of complete and proper plasmid. 30 µL of reaction mix was prepared for each sample as follows: 1 µL PvuI restriction enzyme, 3 µL 10x NEB 3.1 buffer, 3 µL 10x BSA, 2 µg pVenus/pRelax plasmid (23 µL). Each sample was incubated at 37 °C for 2-3 hours.

After incubation, samples were run in a 1% (w/v) electrophoretic gel prepared by 0.5 g of Ultra Pure Agarose (Invitrogen, USA #16500500), 1 µL of Ethidium Bromide (10

mg/mL), and 50 mL of DI water. Gene Ruler™ 1 kb DNA ladder (Fisher Scientific®, Pittsburg, PA) was used as a standard measure.

Nuclear transformation of *C. reinhardtii* wall-deficient strain UTEX 2337 (*CW 15+*)

Plasmid DNA Purification and Preparation

A culture of bacteria DH5α was scaled up to 50 mL of LB medium and grown overnight for 16 hours. Cells were harvest by centrifugation at 6,000 x *g* at 4 °C for 10 min in a 5417-C Eppendorf microcentrifuge. DNA plasmids were purified by using HiSpeed Plasmid Midiprep Kit (QIAGEN, USA # 12643). Purified DNA samples for pVenus and pRelax were eluted into 1.5 mL microcentrifuge tubes and stored at -20 °C to be used for transformation.

Before transformation, plasmid DNA must be linearized to be properly inserted into the nuclear genome. Total 80 µL of reaction mix was prepared for each sample as follows: 1 µL BamHI HF restriction enzyme, 8 µL Cutsmart buffer, 8 µL 10x BSA, 2 µg pVenus/pRelax plasmid (63 µL). Each sample was incubated at 37 °C for 2-3 hours for linearization and subsequently used for transformation.

Transformation by Glass Beads Method

Glass beads method transformation protocol was received from Wipawee Dejtisakdi at University of Maryland Baltimore County. *C. reinhardtii* wall-deficient strain UTEX 2337

(*CW 15+*) was grown in 50 mL of Tris-Acetate-Phosphate (TAP) medium to a cell density of ~5 x 10^6 cells/mL. Cells were pelleted by centrifugation at 6,000 x *g* and resuspended in 5 mL of TAP medium to achieve a cell density of ~50 x 10^6 cells/mL. 300 µL of cells was added to a 1.5 mL microcentrifuge tube to which 2 µg of linearized DNA had already been added. 0.4 mm glass beads were from Sigma (St. Louis, MO Cat# 120M5327V) and were pre-washed and sterilized in acid. 400 µg of acid-washed glass beads were then added to each microcentrifuge tube and each sample was vortexed at top speed for 15 seconds. The solution was carefully pipetted from the beads and spread onto TAP + 1 mg/L bleocin plates for selection. Plates were air-dried in the hood and placed under low light (200 µEinstein) and monitored for colony formation for 7 days.

Transformation by Electroporation

Electroporation transformation protocol was from Shimogawara, *et al* [42]. *C. reinhardtii* wall-deficient strain UTEX 2337 (*CW 15+*) was grown in 200 mL of TAP to a density of 1-3 x 10^6 cells/mL. Cells were chilled on ice for 10 min and then subsequently centrifuged at 2,000 x *g* for 5 min at 4 °C. After the supernatant was disposed, the pelleted cells were resuspended with 1 mL of TAP + 60 mM Sucrose (Sigma, St. Louis, MO, SKU# 252603) to a density of 4 x 10^8 cells/mL on ice. 250 mL of resuspended cells were mixed on ice with 1 µg of plasmid DNA in a 4 mm chilled cuvette (Bio-Rad, Cat# 165-2081) and subsequently incubated for 5 min in 16 °C water bath. Electroporation was performed using a Bio-Rad Total Cell system, BioRad Gene Pulser II (Bio-Rad, USA), with the following parameters: one pulse, 0.8 kV, 25 mF, no resistance, and time constant of 5-6

msec. After electroporation, the cuvettes were incubated at room temperature for 10 min. Cells were gently resuspended and transferred to a 50 mL sterile disposable tube. The cells were allowed to recover for 24 hr by incubating in 10 mL of TAP + 60 mM Sucrose under low light conditions. On the second day, the cells were pelleted at 2,000 x *g* for 1 min at room temperature and resuspended in 2 mL of TAP with 1 mg/L bleocin antibiotic for selection. 500 µL of cells were plated onto TAP + 1.5 mg/L bleocin agar plates and allowed to recover under low light conditions. The plates were monitored for 1 to 2 weeks to see colony formation in the case of successful transformation.

RESULTS & DISCUSSION

pVenus and pRelax Plasmid DNA Purification from Glycerol Stocks

Plasmid DNA was purified and analyzed by a restriction enzyme digest diagnostic. Enzyme PvuI was used because it digested the plasmid at three sites, with a clear comparison of band lengths between the pVenus and pRelax plasmids. The results of the diagnostic digest is shown below (*see Figure 2*):

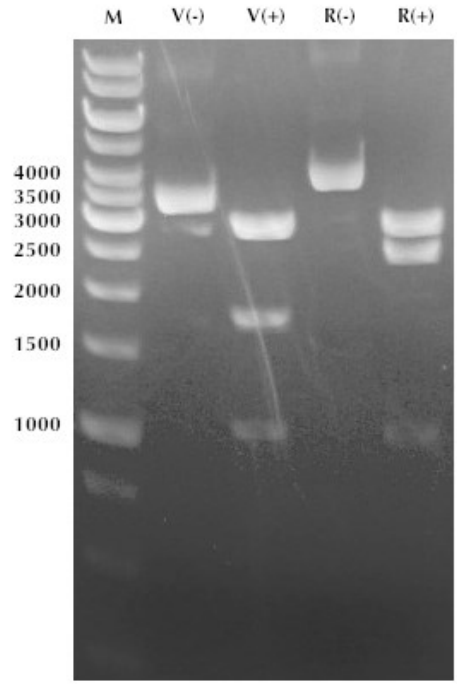

Figure 2: Diagnostic digest analysis of pVenus and pRelax plasmids. From left to right: M, 1 kb marker; V(-), undigested pVenus plasmid; V(+), digested pVenus plasmid; R(-), undigested pRelax plasmid; R(+), digested pRelax plasmid.

The expected sizes of fragments using restriction enzyme, PvuI, were 2929, 1777, and 1045 bp for pVenus and 2929, 2484, and 1045 bp for pRelax. As shown in Figure X above, the diagnostic digest shows a band at the expected sizes for each respective plasmid. The digest confirms that the plasmid purification was successful and also that the plasmids from the glycerol stocks were in fact pVenus and pRelax. With sufficient quantities of plasmid DNA for pVenus and pRelax now purified and readily available, we were able to proceed with attempting a nuclear transformation of *C. reinhardtii*.

Nuclear transformation of C. reinhardtii wall-deficient strain UTEX 2337

Transformation of *C. reinhardtii* wall-deficient strain UTEX 2337 (*CW 15+*) with the glass beads protocol failed to produce any viable transformants (results not shown). The electroporation method was performed twice, on separate occasions. After growing for 1 to 2 weeks in low-light conditions, the plates from the first electroporation transformation also failed to show any successful transformants (*see Figure 3*).

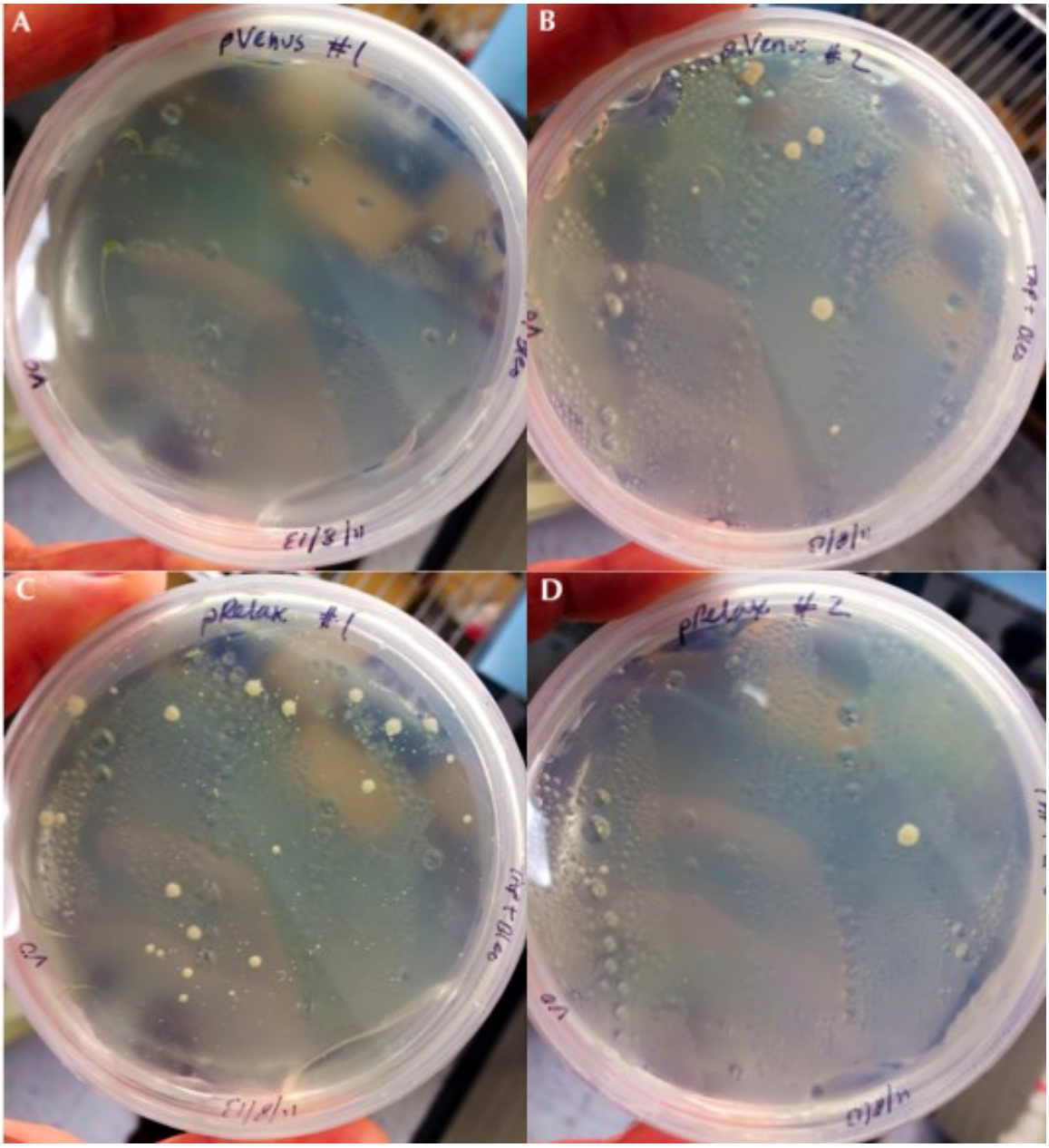

Figure 3: *C. reinhardtii* wall-deficient strain (*CW 15*$^{-}$) UTEX 2337 transformants by electroporation (first run) - Day 7. Electroporation parameters: one pulse, 0.8 kV, 25 mF, no resistance, and time constant of 5-6 msec. (A) – (B) are pVenus transformants. (C) – (D) are pRelax transformants.

The plates labeled pVenus#2, pRelax#1, and pRelax#2 appear to be contaminated with bacteria, despite the plates having bleocin antibiotic. No plates have sign of any viable algal cells or colonies.

The electroporation method was repeated with a higher density of cells transformed, and this time a double restriction enzyme digest using NotI and ApaI sites was performed to linearize plasmid DNA. Plates were observed for 7 days (*see Figures 4a and 4b*).

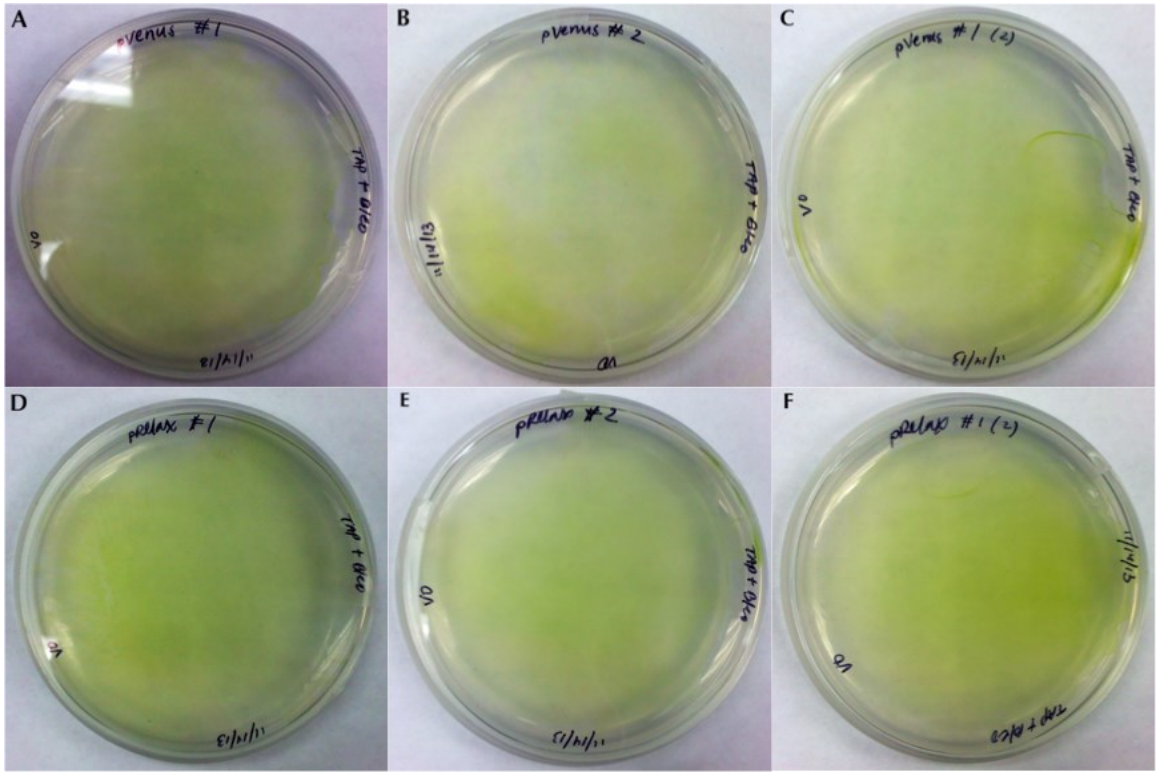

Figure 4a: *C. reinhardtii* wall-deficient strain (*CW 15*$^{+}$) UTEX 2337 transformants by electroporation (second run) - Day 2. Electroporation parameters: one pulse, 0.8 kV, 25 mF, no resistance, and time constant of 5-6 msec. (A) – (C) pVenus transformations labeled pVenus#1, pVenus #2, and pVenus#3, respectively. (D) – (F) pRelax transformants labeled pRelax#1, pRelax#2, and pRelax #3, respectively.

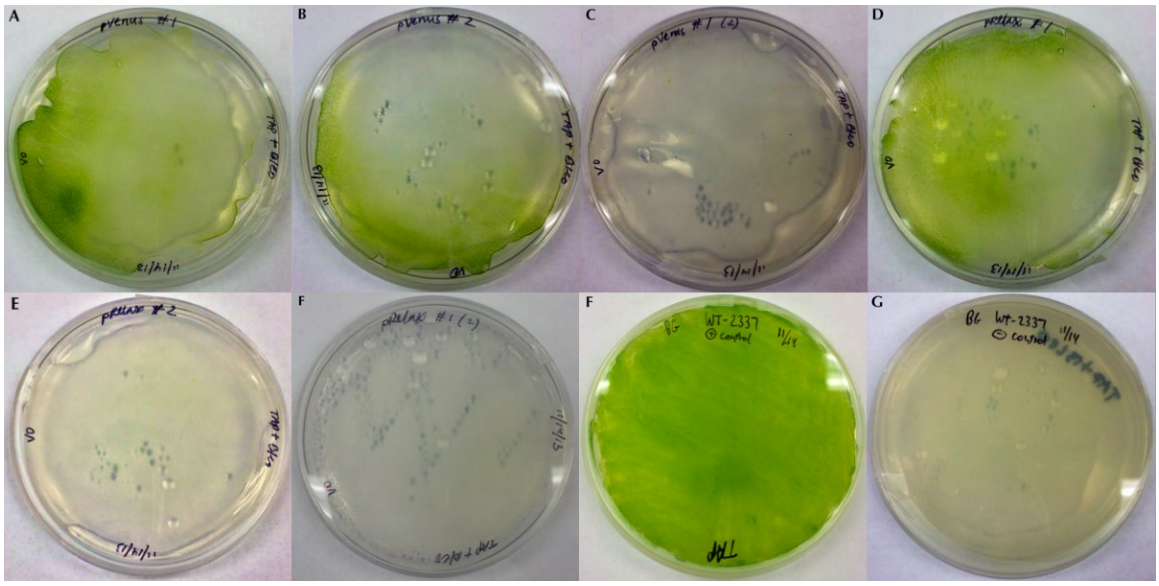

Figure 4b: *C. reinhardtii* wall-deficient strain (*CW 15*$^{-}$) UTEX 2337 transformants by electroporation (second run) - Day 7. (A) – (C) pVenus transformations labeled pVenus#1, pVenus #2, and pVenus#3, respectively. (D) – (F) pRelax transformants labeled pRelax#1, pRelax#2, and pRelax #3, respectively. (F) Positive control with UTEX 2337 on TAP. (G) Negative control with UTEX 2336 on TAP + bleocin.

As shown in Figure 4b above, plates labeled pVenus#3, pRelax#2, and pRelax #3 show no sign of viable cells or colonies after 7 days. Positive control of UTEX 2337 show viability of un-transformed cells, and negative control shows the efficacy of the bleocin antibiotic for successful transformants selection purposes. Plates labeled pVenus#1, pVenus#2, and pRelax#1 appear to have viable cells, however it was impossible to select for individual colonies. A streak of cells was taken from each of the plates with viable cells, and suspended in 10 mL of TAP media + 1 mg/L bleocin to see if the cells were in fact resistant to the bleocin. However, none of the suspended cultures grew in suspended culture.

CONCLUSION

Microalgae are a promising alternative to conventional recombinant protein expression systems, which are vastly expensive and limited in functionality. While there is great potential for microalgae as a molecular farming platform, inconsistent transgene expression hinder microalgae from becoming a standard expression system. The nuclear genome is especially promising for its ability for post-transcriptional, post-translational modifications, and post-translational targeting to specific intracellular organelles, which are necessary for complex protein expression. However, like most eukaryotic organisms, microalgae suffer from unpredictable expression of introduced transgenes as transgenes inserted into the nuclear genome are frequently silenced.

Here we attempted the insertion of transgenes into the nuclear genome of *C. reinhardtii* wall-deficient strain UTEX 2337 (*CW 15+*) using a glass beads method and electroporation method. Transformations with either method failed to yield any positive transformants or results. The failure to produce any successful transformants with the pVenus and pRelax vector may very well be due to an error in the protocol, or execution of the protocol. However, the electroporation method was done twice, both times meticulously, and with several duplicate samples to amplify the possibility of successful transformants. This set of experiments, provided important experiences highlighting the difficulty of successfully introducing transgenes into the nuclear genome of *C. reinhardtii* and yielding high nuclear expression. These difficulties were present, despite the use of strong promoters and good plasmid design. Optimization of "upstream" parameters are a powerful way to improve

transgene expression in microalgae and holds great potential in re-defining microalgae's role in the recombinant biopharmaceutical industry. However, the results of this study show a need for a coupled effort to optimize the "downstream" side of the process to further realize the potential of microalgae systems. It is with this intention that the supplementation of culture medium with sodium butyrate to induce gene expression is studied and discussed in the following chapter of this thesis.

CHAPTER TWO: THE EFFECT OF SODIUM BUTYRATE ON MICROALGAE *CHLAMYDOMONAS REINHARDTII*

One of the main objectives in molecular farming is the achievement of high recombinant protein production. While the mechanism of gene silencing is not clearly understood, the role of chromatin structure has been identified as an influencing factor. Two types of gene silencing are distinguished: transcriptional silencing, which involves the inhibition of in transgene transcription, and post-transcriptional gene silencing, which is characterized by the rapid degradation of initially synthesized transcripts [51]. Many avenues have been examined in the "upstream" side of process engineering and design, such as codon optimization, promoters, transformation-associated genotypic modifications, enhancer elements, regulatory mechanisms, and sensitivity to proteases and protein localization. While these factors that can be precisely controlled through the design of the plasmid-construct, there are still many unpredictable factors that inhibit transgene expression. Additional to these upstream parameters, the cultivation operating regulations, such as mixing, illumination, media composition, pH, temperature, and nutrient concentration, can greatly influence protein yields [31]. Sodium butyrate has been well documented to arrest cell division and increase gene expression in both mammalian and plant systems [52]. These changes present opportunities for higher production levels of the protein of interest, while reducing the quantity of cells needed to more manageable densities and increasing the productive life of the cultures.

BACKGROUND

There is a wealth of research and literature on the effect of sodium butyrate on mammalian and plant cells in culture. Sodium butyrate has been shown to cause a variety of morphological and functional changes in these cells, often related to cell shape, cell growth, and gene expression. It is also known to induce apoptosis in some cell lines [53]. Butyric acid is a 4-carbon fatty acid that is naturally formed in the body, but is toxic to human cells in culture at concentrations above 10 mM [54].

Sodium butyrate induces cell-growth arrest, apoptosis, and morphological changes in mammalian and plant cells in culture

Decades of research has shown that sodium butyrate arrests cells at the G1 to S phase transition point of the cell cycle for many mammalian cells [52]. A study in 1973 by Wright showed that CHO cells grown in the presence of sodium butyrate decrease their growth rate, increase in length, and have a tendency to grow in a monolayer [55]. The treated cells had a distinctly longer and more "fibroblast-like" characteristic compared to cells cultured in the absence of sodium butyrate. The doubling times were increased by nearly 100% in the presence of 0.5 mM and 1.0 mM sodium butyrate. These morphological and cell growth changes were observed to be slowly reversible after the culture medium was replaced with fresh growth medium. An impressive review by Prasad and Sinha in 1976, documents the effects of sodium butyrate on the mammalian cells in cultures. The report goes to show that sodium butyrate reversibly inhibits the division of mouse neuroblastoma cells and increases the intracellular level of adenosine 3', 5'-cyclic monophosphate (cAMP).

The effect was slightly different on human neuroblastoma cells as it caused extensive cell death and induced neurites along with inhibiting cell growth. The growth rate, and morphology of human tumor neuroblasts or human tumor astrocytes were unaffected at concentrations under 0.5 mM, but apoptotic at higher concentrations. The normally round HeLa cells become spiky in the presence of 2.5 – 5 mM sodium butyrate. The growth rate of rat XC sarcoma line cells was not affected by 1.0 mM sodium butyrate, but cells were observed to be considerably flattened and cellular outline unclear. However, concentrations of 5.0 mM produced no effect on morphology, growth, or differentiation on rat mammary tumor cells or rat myoblast cells. Growth rates of slow growing hepatoma (8999) cells were unaffected by 1.0 mM sodium butyrate, but growth rates of fast growing hepatoma (3924 A) cells were inhibited. Sodium butyrate in concentration of 2.5 mM was observed to inhibit cell division of monkey or calf kidney epithelial cells, and chick embryo cells, with no changes in their morphologies [54].

The effect of sodium butyrate on plant systems is not as extensively studied as mammalian cells. A 1988 study with Jerusalem artichoke (*Helianthus tuberosus* L.) tuber explants, showed that sodium butyrate inhibited DNA replication and cell division [56]. In transgenic tomato (*Lycopersicon esculentum* Mill.) cells, cell growth was hindered at concentration of 5 – 10 mM sodium butyrate and arrested at 20 mM [57].

Sodium butyrate induces transgene expression in mammalian and plant cells

Throughout the past several decades, sodium butyrate has also been shown to induce enhanced gene expression in a variety of mammalian cells. In 1983, Gorman, *et al.*, showed up to a 7.5 fold increase in recombinant chloramphenicol acetyltransferases gene with HeLA and monkey kidney CV-1 cells induced by sodium butyrate [58]. Nearly a decade later, sodium butyrate was used to enhance the expression levels of nine different tissue plasminogen activator analogues in CHO cells. Inductions in the presence of sodium butyrate induced a 2 – 9 fold increase in the production of these nine recombinant proteins, on average [52]. In 1995, Kooistra, *et al.*, discovered that stimulation of tissue-type plasminogen activator (t-PA) expression in human umbilical vein endothelial cells (HUVEC) by sodium butyrate induction was related with histone H4 acetylation [59].

Interestingly, sodium butyrate has a similar effect on plant cells as well. A relatively recent study in 2001 by Chung, *et al.*, showed a 143% increase in recombinant rotavirus VP6 in transgenic tomato (*Lycopersicon esculentum* Mill.) cells treated with sodium butyrate [57]. Additionally, analysis of total protein extracts of the sodium butyrate-supplemented transgenic tomato cells showed the up-regulation of 14 proteins and down-regulation of 7 proteins. Interestingly, 4 of the up-regulated proteins were similar to proteins specific for cell-growth arrest while 3 down-regulated proteins matched cell division proteins. One of the up-regulated proteins matched a histone acetyltransferase type B catalytic subunit, and two of the down-regulated proteins resembled histone deacetylases, indicating sodium butyrate behaves similarly to a histone deacetyltransferase inhibitor. A similar study was

conducted in 1990 in alfalfa (*Medicago sativa*) cells. The addition of sodium butyrate to the culture revealed that butyrate was metabolized, which lead directly to histone acetylation [60].

Although the exact mechanism behind enhanced gene expression by sodium butyrate induction is still ambiguous, it is clear from previous literature and research that sodium butyrate is capable of initiating changes in chromatin structure as a result of hyperacetylation of histones [52].

The role of histone acetylation in gene expression

Nuclear DNA exists as a system of chromatin structures, resulting in compaction of the nuclear DNA about 10,000-fold. This orderly packing of DNA in in the nucleus plays an important role in the functional aspects of gene regulation [61]. A repeating structure of nucleosome core particles makes up the chromatin. 146 bp of DNA wrap around the histone octamer core of the nucleosome, while linker DNA of varying lengths join each nucleosome. There are four core histone domains H3, H4, H2A, and H2B, each with a basic N-terminal domain, a histone fold, and a C-terminal domain [62]. The so called N-terminal tails of the core histones consist of 16 – 44 amino acids and are the sites of various post-synthetic modifications, which include acetylation, phosphorylation, methylation, ubiquitination, glycosylation, and ADP-ribosylation [61]. Acetylation of the nucleosome inhibits the higher order folding of the chromatin, preserves the unfolded structure of the transcribed nucleosome, and induces the solubility of chromatin,

ultimately leading to increased exposure of DNA to transcription factor binding [61, 63, 64].

In 1977, Allfrey, *et al.*, first discovered the correlation between high levels of histone acetylation and gene transcription [65]. Within a decade, it was observed that histone acetylation is dynamic; meaning a localized shift in the dynamic equilibrium between histone acetyltransferases and histone deacetyltransferases activities towards acetylation results in a localization of highly acetylated chromatin on or near transcriptionally active genes [66, 67]. The roles of H3 and H4 core histones have been studied extensively by using specific antibodies in the past several decades, confirming the correlation between high acetylation and gene transcription [68].

Histone acetylation in Chlamydomonas reinhardtii

In unicellular green algae *C. reinhardtii*, the main target of acetylation is histone H3. Half-life for acetylation of H3 was found to be 1.5 – 3 min, when dynamically acetylated to 30% [69]. In contrast, histone acetylation has a turnover half-life of 3 – 30 min in animal cells and 30 – 300 min in yeast [69]. The majority of studies of histone acetylation have been performed in animal cells, in fungi like *S. cerevisiae* or protists like *Tetrahymena*, where the H4 histone is the primary target of histone acetylation. In higher plants, histone H3 is the predominant target of histone acetylation; especially those localized in transcriptionally active chromatin domains, followed by histone H4. However, in *C. reinhardtii*, the difference is drastic and steady-state levels of multi-acetylated H3 are very high [69].

Mammalian Bcl-x_L protein and its role in inhibiting cell death

The Bcl-x_L protein is a member of the B-cell lymphoma (Bcl) family responsible for apoptosis in a cell and is localized to the mitochondria. Briefly, members of the Bcl-2 family either act as apoptosis enablers or apoptosis inhibitors by recruiting proteins from the caspase (cysteine-aspartate specific protease) superfamily [70]. The specific role of Bcl-x_L is to indirectly inhibit the release of cytochrome c, which led to activation of downstream "executioner" caspases that trigger cell apoptosis [71]. Bcl-xL has been shown to inhibit apoptosis and increase tolerance to environmental stress in various mammalian cell types and plant cells (*see references for more detailed overview of the Bcl-xL protein*) [49, 72, 73, 74]. The protein is hypothesized to have similar functionality when introduced to microalgae.

MATERIALS & METHODS

Sodium butyrate induction of C. reinhardtii wall-deficient strain

Sodium n-butyrate (>98.5% purity) was from Sigma (Sigma-Aldrich, MO, USA, SKU# B5887). It was dissolved in TAP medium as a 1 M stock solution. The stock solution was stored at -20 °C and diluted to appropriate concentrations with TAP medium immediately before inducing the cells. *C. reinhardtii* cell wall-deficient strain UTEX 2337 was grown to a density of 1 x 10^7 cells/mL in TAP medium in a T-25 flask. Ten T-25 flasks were seeded at a density of 2.5 x 10^5 cells/mL and grown under normal conditions in TAP media on a rotary shaker. Cell counts were taken approximately every 12 hours using Guava Personal

Cell Analysis (PCA) Base System (Millipore, USA, Cat# 0500-1090). Samples were diluted to appropriate concentrations in Dulbecco's phosphate-buffered saline (DPBS) balanced salt solution before counting.

After 45 hours from inoculation, cell densities were around 1 x 10^6 cells/mL. Cells were pelleted by centrifugation at 6,000 x *g* for 5 min at room temperature. The supernatant was disposed and the pellet was resuspended in 10 mL of TAP + varying concentrations of sodium butyrate (0 mM, 50 mM, 100 mM, 250 mM, and 500 mM) and grown under normal illumination on a rotary shaker. Cells were observed at 100x in a Nikon Eclipse *Ti* microscope at 24 hrs and 48 hrs after sodium butyrate induction.

45 hours after sodium butyrate induction, the cells were harvested by centrifugation at 6,000 x *g* for 10 min at room temperature. Cell pellets were stored at -80 °C in the case they were needed for further analysis.

Colony PCR of pRelax #6 and #7

Two C. *reinhardtii* cell wall-deficient Venus-Bcl-x_L (pRelax) strains were provided on TAP + 1 mg/L bleocin antibiotic plates by Junaid Faruq at the Johns Hopkins University. A small quantity of each plate was streaked and resuspended in 50 µL of Tris EDTA (TE) Lysis Buffer (0.01 M Tris-HCl (pH 8.0), 0.1 M EDTA). Samples were incubated at 100 °C for 5 min and subsequently cooled in a fridge to 4 °C. The cells were then centrifuged at 10,000

x *g* for 10 min. The supernatant, now containing extracted DNA and RNA, was collected to be used directly to obtain the DNA template for PCR.

PCR reaction was mixed following the Phusion® High-Fidelity DNA Polymerase (New England Biolabs, Ipswich, MA #M0530) protocol. 20 μL reaction mixtures were made for pRelax #6, pRelax #7, and pRelax plasmid for positive control as follows: 10 μL Nuclease-free water, 4 μL of 5x Phusion® HF, 0.4 μL of 10 mM dNTPs, 0.6 μL of DMSO, 0.2 μL of Phusion® DNA Polymerase, 1 μL of forward primer, 1 μL of reverse primer, and 2 μL of genomic DNA (1 μL for plasmid DNA). Forward primer sequence was 5'-TATCTCGAGATGGTGTCG-3' and reverse primer sequence was 5'-ATAAGATCTTCAGGCGCGCTTAC-3'. Samples were placed in an Mastercycler Personal PCR machine (Eppendorf, New York, USA) for a total of 34 PCR cycles with each cycle set as: 2 min at 95 °C, 20 sec at 95 °C, 45 sec at 52 °C, 1 min at 72 °C, 10 min at 72 °C, and ending at 4 °C.

After completion of 34 cycles of PCR, the samples were run in a 1% (w/v) electrophoretic gel prepared by 0.5 g of Ultra Pure Agarose (Invitrogen, USA #16500500), 1 μL of Ethidium Bromide (10 mg/mL), and 50 mL of DI water. Gene Ruler™ 1 kb DNA ladder (Fisher Scientific®, Pittsburg, PA) was used as a reference.

Sodium butyrate supplementation of pRelax

C. reinhardtii cell wall-deficient Venus-Bcl-x_L (pRelax) strain were seeded at a density of 5.0 x 10^5 cells/mL and grown under normal conditions in TAP media on a rotary shaker. Cell counts were taken approximately every 12 hours using Guava Personal Cell Analysis (PCA) Base System (Millipore, USA, Cat# 0500-1090). Samples were diluted to appropriate concentrations in Dulbecco's phosphate-buffered saline (DPBS) balanced salt solution before counting and also Guava Viacount reagent (Millipore, USA, Cat# 4000-0040) for more accurate counting and apoptosis analysis.

After around 21 hours from inoculation, cell densities were around 1 x 10^6 cells/mL. Cells were induced with sodium butyrate with the same procedure outlined above for wild-type wall-deficient strain. Cells were observed at 100x in a Nikon Eclipse *Ti* microscope at 24 hrs and 48 hrs after sodium butyrate induction. Cells were also observed for fluorescence under a confocal microscope using a Zeiss LSM 510 Meta confocal microscope at 20x magnification.

57 hours after sodium butyrate induction, the cells were harvested by centrifugation at 6,000 x *g* for 10 min at room temperature. Cell pellets were washed with DPBS, re-pelleted by centrifugation at 6,000 x *g* and stored at -80 °C for subsequent protein extraction and analysis.

Extraction of Venus-Bcl-x_L protein

Pelleted cells were taken from -80 °C and defrosted at room temperature. Cells were washed in 25 mM K_2HPO_4/KH_2PO_4 (pH 7.0) and centrifuged at 500 x *g* for 10 min. Each sample was resuspended in 1 mL of Algae Lysis Buffer (50 mM Tris-HCl (pH 8.0), 500 mM NaCl, 0.1% Tween20) with *c0mplete*, Mini, EDTA-free protease inhibitor cocktail (Roche, USA, Cat# 11 836 170 001). The samples were then sonicated on ice for 6 x 30 second rounds with 1 minute intervals. Sonication was done at 55 W to avoid foaming. After cell lysis, samples were centrifuged at 7,500 rpm. The supernatant was extracted and stored at -80 °C to be used later for SDS-PAGE.

Western blot on Venus-Bcl-x_L protein

Protein extracts were taken from -80 °C and defrosted at room temperature. Prepared a 2x sample buffer containing 50 µL β-mercaptoethanol (BME) and 950 µL 2x Laemmli sample buffer (BioRad, USA, cat# 161-0737). 25 µL of each sample was taken and mixed with 25 µL of the 2x sample buffer mix and boiled at 100 °C for 5 – 10 min to denature proteins to primary and secondary structures. Samples were then loaded into an SDS-PAGE gel and run at 130 V for around 75 min in SDS-PAGE running buffer. Gel was transferred onto a PVDF membrane by running at 100 V for 75 min in transfer buffer. The membrane was blocked for any non-specific binding with a solution of 5% blotting grade dry milk powder (BioRad, USA) in PBST (Phosphate-Buffered-Saline-Tween20) by rotating on a shaker for 1 hr at room temperature. The membrane was washed with PBST. Two membranes were treated with two separate primary antibodies: GFP (4B10) Mouse mAB (Cell Signaling

Technology, USA, Cat# 2955) and Bcl-X_L Rabbit monoclonal antibody (mAb) (Cell Signaling Technology, USA, Cat# 2764). The antibodies were diluted at 1:2000 (GFP) and 1:1000 (Bcl-x_L) in 6 mL of PBST with 1% dry milk. The membranes were incubated with each primary antibody solution overnight at 4 °C with gentle agitation. The second day, membranes were washed three times for 5 minutes each with 10 mL of PBST. Each membrane was then incubated with the appropriate HRP-conjugated secondary antibody, anti-mouse (GFP) and anti-rabbit (Bcl-x_L), with gentle agitation for 1 hr at room temperature. The membranes were then developed using a Western-C developing kit (BioRad, USA).

RESULTS

Sodium Butyrate inhibits growth rate and induces apoptosis in wild-type *C. reinhardtii*

Wild-type C. *reinhardtii* cell wall-deficient strain UTEX 2337 was grown in TAP and induced with varying concentrations of sodium butyrate after 45 hrs of inoculation. Two identical sets of experiments were run in parallel, set A and set B, for comparison. Cell counts were done for both sets A and B, every 12 hours and recorded. We found that a concentration of 50 mM sodium butyrate slightly inhibited cell growth, while a concentration of 100 mM sodium butyrate significantly inhibited cell growth compared to the untreated cells. Concentrations of 250 mM and 500 mM were immediately lethal for the cells and cell viability and cell growth dropped drastically upon induction (*see Figures 5a and 5b*).

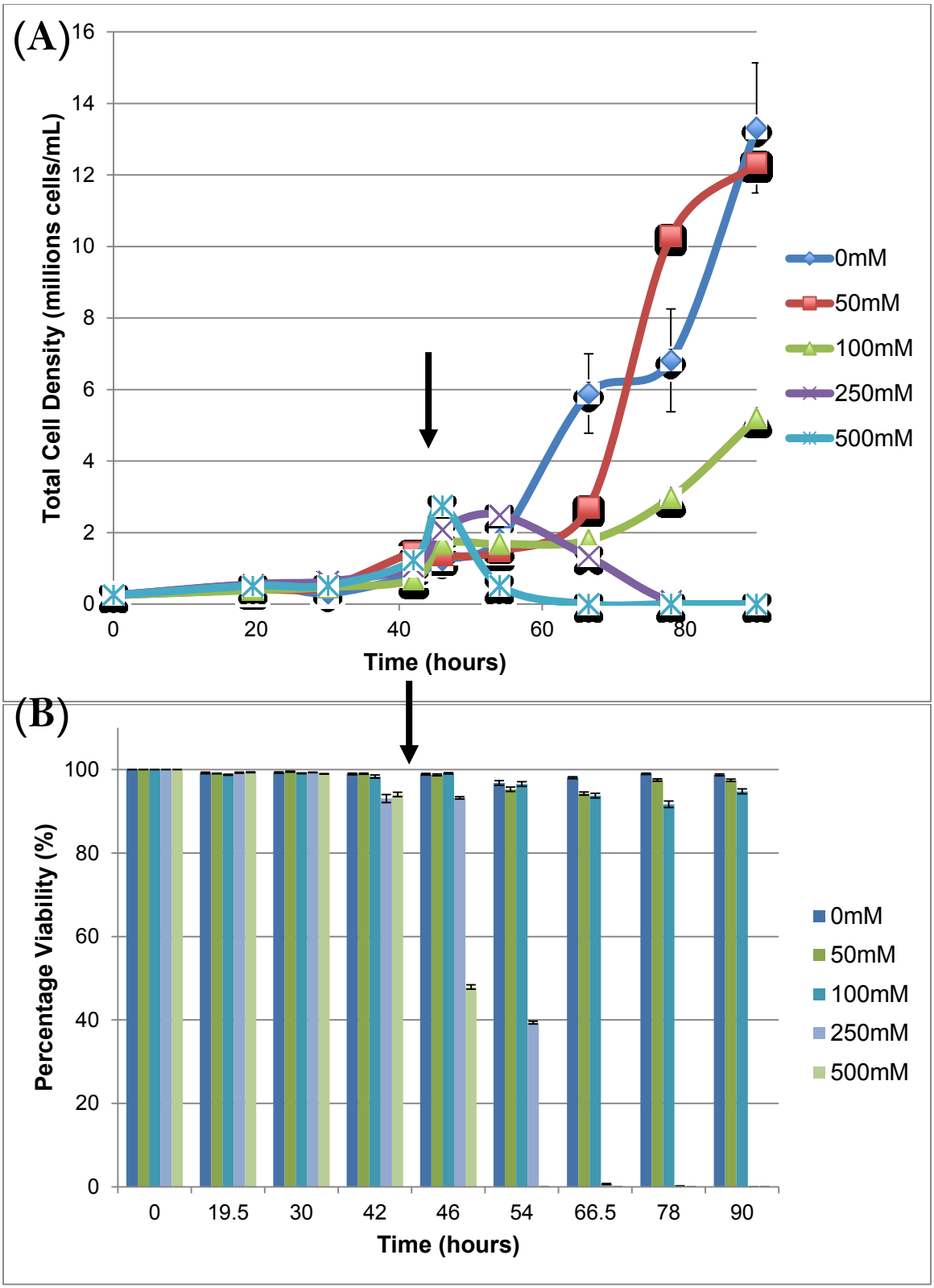

Figure 5a: Effect of sodium butyrate on *C. reinhardtii* wall-deficient strain (*CW 15+*) UTEX 2337 – Set A. Sodium butyrate induction point was 45 hours after inoculation (indicated by arrow). (A) Cell density vs. time (B) Cell viability vs. time

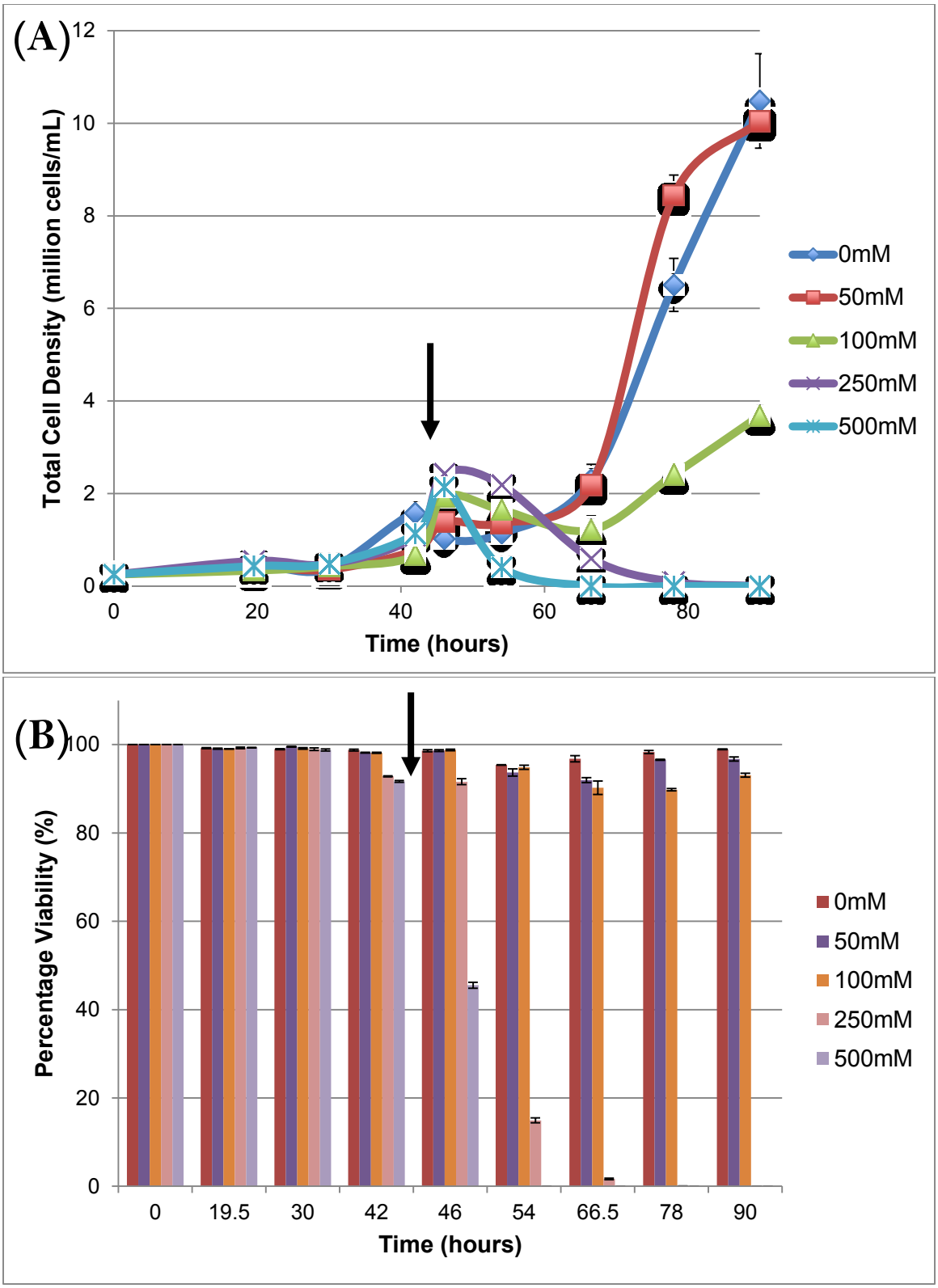

Figure 5b: Effect of sodium butyrate on *C. reinhardtii* wall-deficient strain (*CW 15+*) UTEX 2337 – Set B. Sodium butyrate induction point was 45 hours after inoculation (indicated by arrow). (A) Cell density vs. time (B) Cell viability vs. time

The cultures were supplemented with sodium butyrate when the cell density reached about 1 x 10^6 cells/mL and when the cells started to enter the exponential growth phase. As shown in Figures 5a and 5b above, control cells grew as normal and displayed expected exponential growth behavior. Cells treated with 50 mM sodium butyrate also displayed exponential growth behavior, and in both cases grew faster than the control group. At 90 hours, however, the cell densities of the control group and 50 mM group hovered around 10-13 x 10^6 cells/mL and the percentage difference between cell densities of 50 mM from the control was 7.41% and 4.17% for sets A and B, respectively. In both cases the control group began to outgrow the 50 mM group, as the 50 mM group seemed to reach a plateau phase. This is within the standard error range for the control group. A concentration of 50 mM sodium butyrate briefly arrested the cell growth in both cases, although the cells seemed to recover within 24 hours. A concentration of 100 mM also arrested cell growth upon induction, but the cells appeared to slowly recover after 36 hours and enter a less drastic exponential phase compared to the control and 50 mM cells. The percentage difference in final cell concentration between cultures treated with 100 mM and 0 mM were 60.99% and 64.85% for sets A and B, respectively. Cells treated with 250 mM and 500 mM sodium butyrate had a significant reversal in cell growth and the cell density of the culture quickly dropped below detectable traces.

Also shown in Figures 5a and 5b above, is the effect of sodium butyrate on the viability of the cells. Cell viability was above 95% prior to sodium butyrate induction for all cultures, indicating that the cells were healthy. A concentration of 50 mM showed a drop in cell

viability to 93.77% and 91.97% for sets A and B, respectively, at 66.5 hours (20.5 hours post sodium butyrate induction). 100 mM showed a slightly more noticeable decrease as viability dropped to 91.7% and 89.8% for sets A and B, respectively. Cell viabilities for 50 mM and 100 mM slowly recovered after 24 hours, albeit more slowly for 100 mM. Final percentage differences for cell viability between control and 50 mM were 1.32% and 2.22% for sets A and B, respectively. Final percentage differences for cell viability between control and 100 mM were 4.02% and 5.93% for sets A and B, respectively. A concentration of 500 mM dropped cell viability below 50% within the first hour after induction and the cells were completely dead within the first day. A concentration of 250 mM had less immediate results, but showed to reduce cell viability to under 20% after 24 hours of induction. The cells never recovered, and by the second day the cells were dead.

The effect of sodium butyrate on the algae cells was also visible to the naked eye. The suspension cultures grown in T-25 flasks can change in appearance depending on the cell density and viability of the cultures (*see Figure 6*).

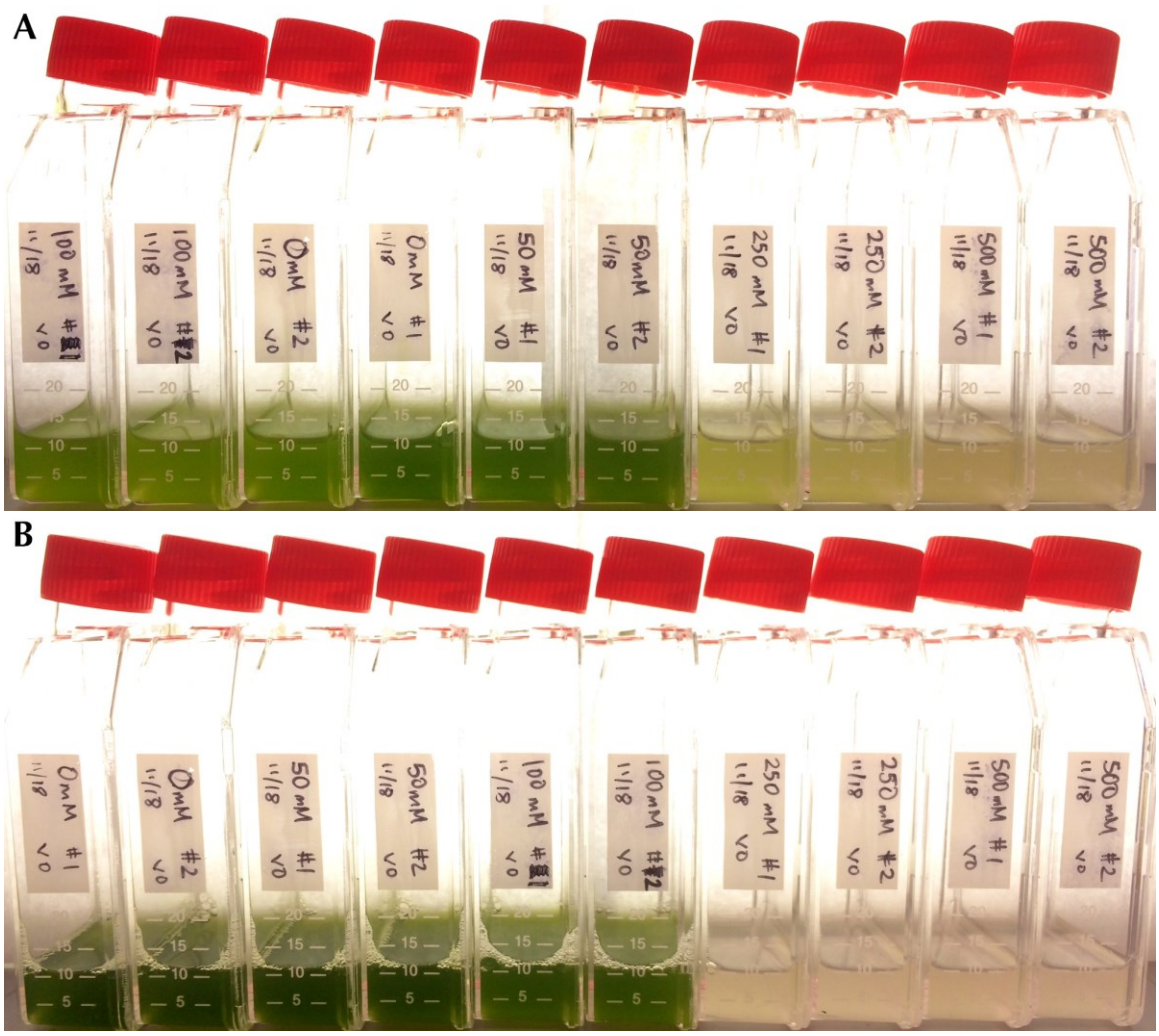

Figure 6: *C. reinhardtii* wall-deficient strain (*CW 15+*) UTEX 2337 treated with sodium butyrate. From left to right: TAP + 0 mM sodium butyrate, TAP + 50 mM sodium butyrate, TAP + 100 mM sodium butyrate, TAP + 250 mM sodium butyrate, TAP + 500 mM sodium butyrate. (A) 1 day after sodium butyrate supplementation. (B) 2 days after sodium butyrate supplementation.

1 day after sodium butyrate induction, cultures induced with 250 mM and 500 mM were already beginning to pale. By the second day, the cultures had turned completely white indicating that the cells were dead. This is in stark contrast with the dark green color of the healthy control cells, which were untreated. The retardation of cell growth for cells treated with 100 mM sodium butyrate is visualized as well. After sodium butyrate induction, cultures supplemented with 100 mM sodium butyrate maintain a bright green color and

only slightly darken in comparison to untreated cultures and cultures grown in 50 mM sodium butyrate.

Sodium butyrate induces morphological changes in wild-type *C. reinhardtii*

A microscopic view of the cultures also showed interesting implications of the effect of sodium butyrate on the algae cell, even within an hour of induction (data not shown). Untreated cells and cells treated with 50 mM sodium butyrate appeared to behave normally and were very active (data not shown). Cells treated with 100 mM, and above, showed significant reduction in mobility and appeared "frozen." Cells were monitored under the microscope for 2 days after sodium butyrate induction (*see Figure 7*).

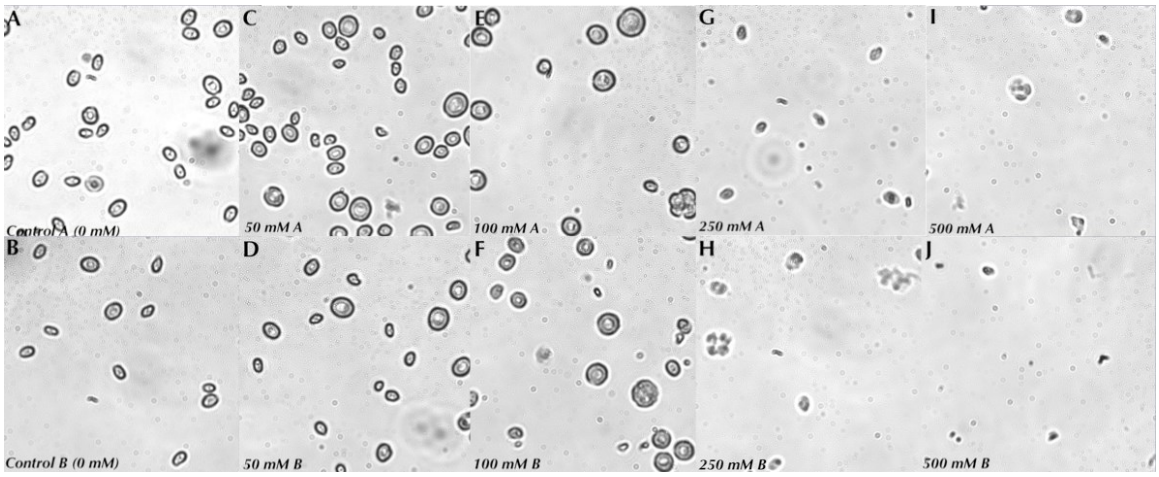

Figure 7: Effect of sodium butyrate on cell growth and morphology 1 day after induction. *C. reinhardtii* wall-deficient strain (*CW 15+*) UTEX 2337 taken at 20X magnification. (A) control 0 mM A (B) control 0 mM B (C) 50 mM A (D) 50 mM B (E) 100 mM A (F) 100 mM B (G) 250 mM A (H) 250 mM B (I) 500 mM A (J) 500 mM B

Cells treated with 50 mM sodium butyrate had a tendency to cluster compared to untreated cells. However, cell mobility appeared normal and cells were very active like the

cells in the untreated control group. Cells also appeared slightly larger than the control group. Cells treated with 100 mM sodium butyrate were minimally active and significantly larger than untreated cells. Although cell mobility was reduced significantly, it seemed that the cells had slightly recovered some mobility compared to their "frozen" state 1 hour after sodium butyrate induction. Cells induced with 250 mM sodium butyrate never recovered mobility and had a "shriveled" appearance. Cultures supplemented with 500 mM sodium butyrate had no sign of viable cells, and only had cell debris. By zooming in, we took a closer look at the treated cells (*See Figure 8).*

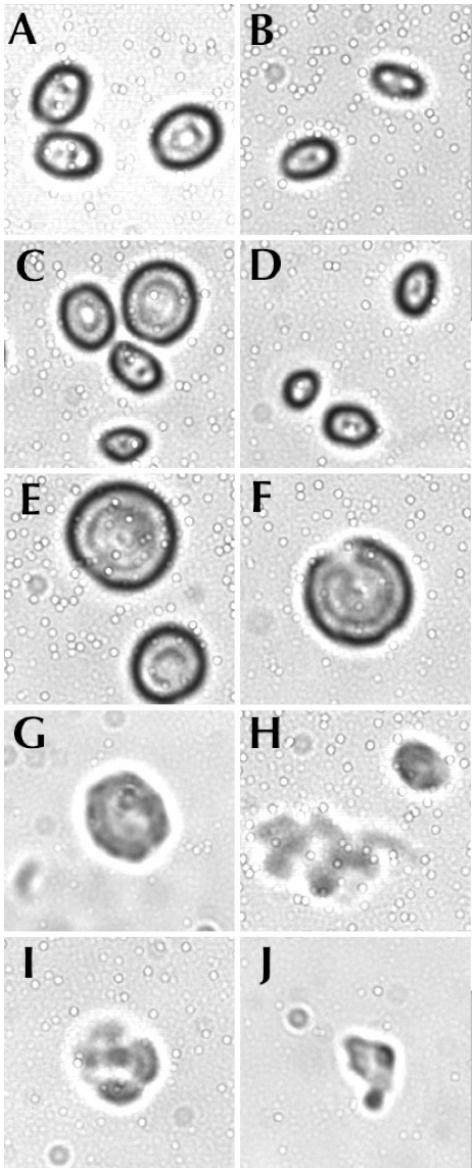

Figure 8: Effect of sodium butyrate on cell growth and morphology 1 day after induction. *C. reinhardtii* wall-deficient strain (*CW 15+*) UTEX 2337 taken at 20X magnification and zoomed. (A) control 0 mM A (B) control 0 mM B (C) 50 mM A (D) 50 mM B (E) 100 mM A (F) 100 mM B (G) 250 mM A (H) 250 mM B (I) 500 mM A (J) 500 mM B

A closer look at the individual cells further emphasizes the changes in extracellular morphology along with the changes intracellularly. Untreated cells are still relatively small at this magnification and a small spot is visible representing the cell nucleus. With the lack of quality of intracellular organelles, it is difficult to see the crescent-shaped chloroplast,

which makes approximately 40% of the cell. As shown in Figure 8 above, a treatment of 50 mM is ineffective in changing the morphology for the majority of the microalgae cells, yet some of the cells are slightly larger with what also seems to be an enlarged nucleus. The changes are significantly more pronounced in cells supplemented with 100 mM. Individual cells seem extremely swollen, however intracellular organelles seem intact, especially the enlarged nucleus. The cells treated with 250 mM and 500 mM show extensive disintegration of the cell membrane and intracellular organelles, leaving only scattered fragments of the cell. The cells treated with 250 mM and 500 mM sodium butyrate are also in stark contrast with the cells treated with 100 mM as they appear small and shriveled, indicating the cells are in the final stages of apoptosis.

The effect of sodium butyrate on a pRelax transgenic *C. reinhardtii*

Colony PCR was performed on wall-deficient C. *reinhardtii* strains pRelax#6 and pRelax#7 to verify the presence of the Venus-Bcl-x_L gene sequence in the nuclear genome (*see Figure 9*).

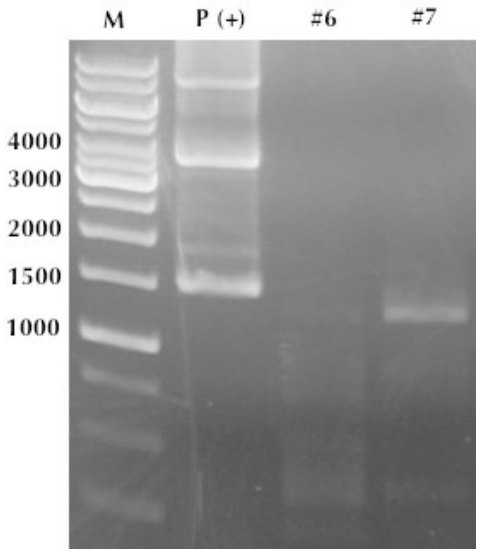

Figure 9: PCR analysis on *C. reinhardtii* wall-deficient strains pRelax #6 and #7. From left to right: M, 1 kb marker; P (+), pRelax plasmid positive control; #6, pRelax strain #6; #7, pRelax strain #7. Expected size of PCR product is 1439 bps.

As shown above in Figure 9, the PCR analysis shows that the pRelax#7 strain has pRelax plasmid present in the nuclear genome. The expected band size for the Venus-Bcl-x_L gene sequence is approximately 1439 bps, and we observe a band at the appropriate location for pRelax#7. Interestingly, pRelax#6 did not appear to have the pRelax gene sequence, despite its resistance to the bleocin resistance. Thus, pRelax#7 was chosen for the subsequent set of sodium butyrate treatment experiments, and is referred to as pRelax from this point on.

pRelax cells were exposed to the same set of concentrations of sodium butyrate exposed to the wild-type *C. reinhardtii* cells. 21 hours after inoculation, five identical cultures were induced with 0 mM, 50 mM, 100 mM, 250 mM, and 500 mM sodium butyrate. Cell counts and cell viability measurements were taken at approximately 12 hour points (*see Figures 10 and 11*).

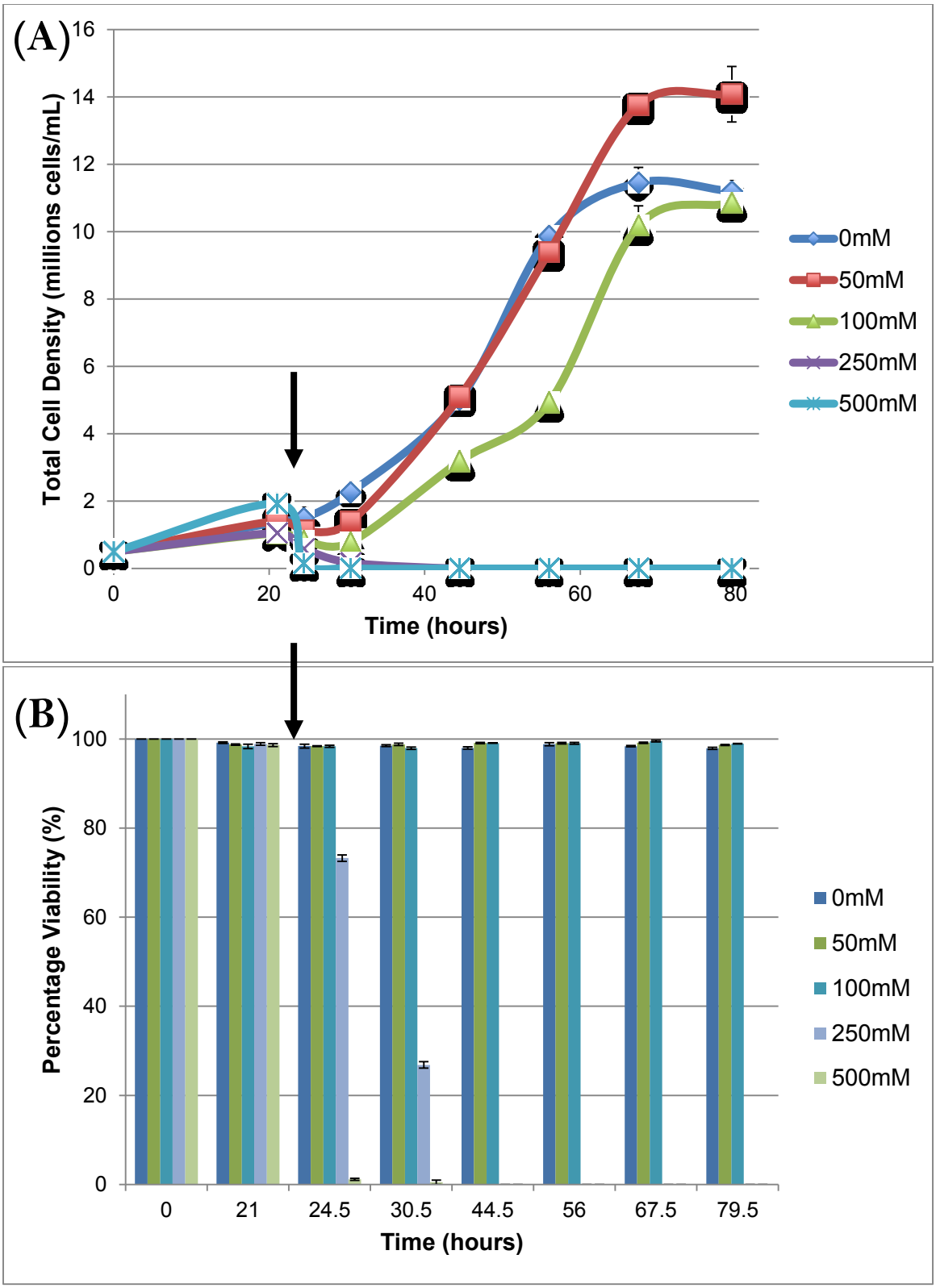

Figure 10: Effect of sodium butyrate on *C. reinhardtii* wall-deficient pRelax strain. Sodium butyrate induction point was 22 hours after inoculation (indicated by arrow). (A) Cell density vs. time (B) Cell viability vs. time

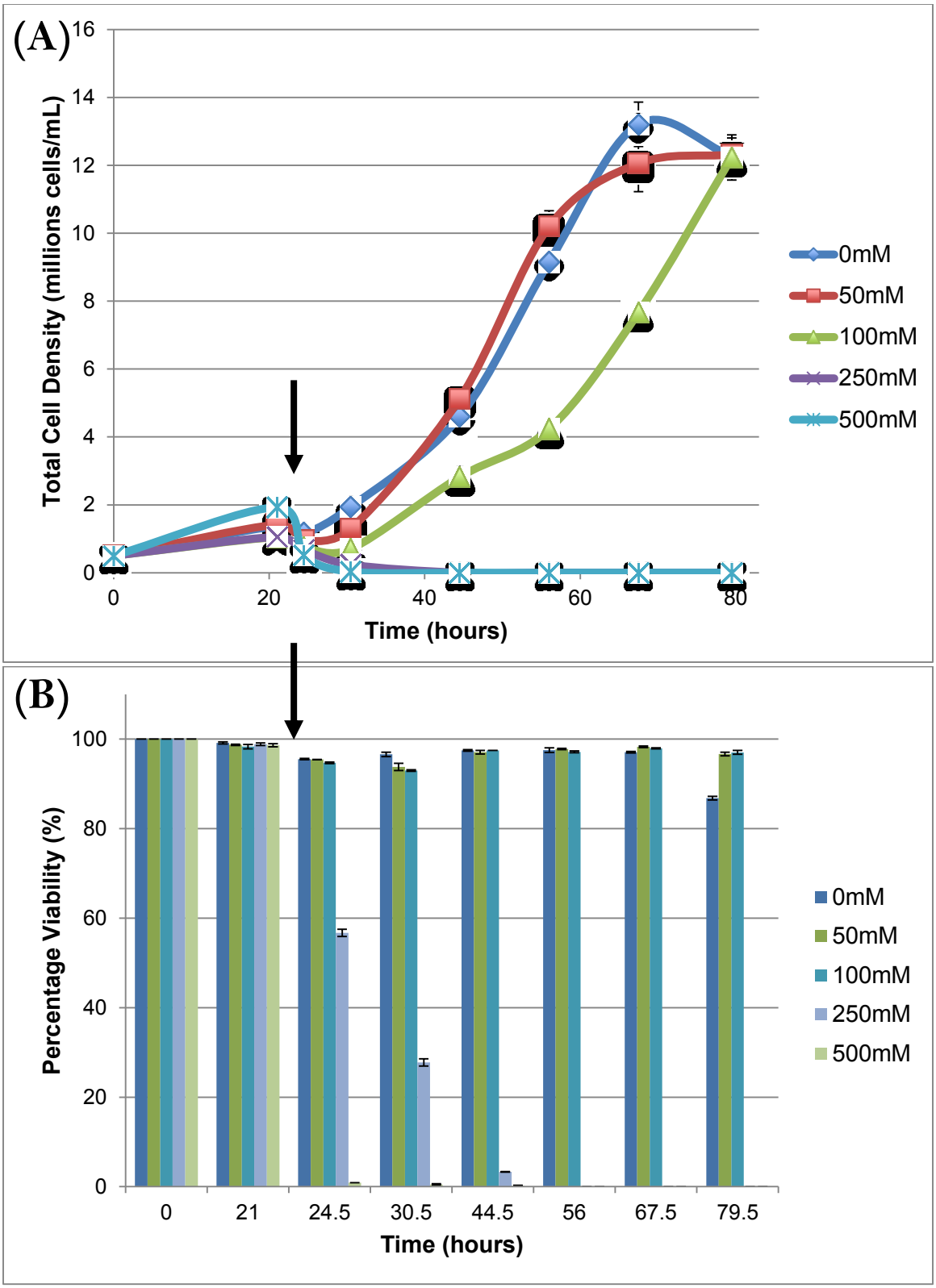

Figure 11: Effect of sodium butyrate on *C. reinhardtii* wall-deficient pRelax strain – Guava Viacount. Sodium butyrate induction point was 22 hours after inoculation (indicated by arrow). (A) Cell density vs. time (B) Cell viability vs. time

Figure 10 represents counts and viability measurements taken with the cells diluted in DPBS while Figure 11 represents counts and viability measurements taken with the cells diluted in Guava Viacount reagent. The red Guava Viacount reagent acts differently by permeating the cell walls and staining the cells, separating the viable cells from the cell debris. Apoptotic and dead cells absorb the orange dye because of the compromised membrane integrity. Therefore, the Guava Viacount reagent is able to separate out the apoptotic cells from the viable cells unlike the DPBS.

Both Figure 10 and Figure 11 show similar results for the resistance of the pRelax strain to inhibition of cell growth and induction of apoptosis by sodium butyrate. We observed that the growth for cells treated with 50 mM sodium butyrate was only slightly inhibited immediately after induction. Cells quickly recovered and maintained growth rates similar to the control untreated cells. Cell treated with 100 mM sodium butyrate experienced a slight shock to sodium butyrate induction, but also quickly recovered and exhibited only a slightly slower growth rate than the control group. Eventually, the cell densities converge at around 12 x 10^6 cells/mL for untreated, 50 mM and 100 mM cells. When measured with Guava Viacount reagent, the final cell density between the control, 50 mM, and 100 mM vary only by approximately 0.3%.

Concentrations above 250 mM of sodium butyrate quickly induced apoptosis in the pRelax cells, which is shown by the sharp drop in cell density and cell viability upon sodium butyrate induction. In the case of the cells treated with 50 mM and 100 mM

sodium butyrate, the cell viability never drops below 97% when measured with DPBS and 93% when measured with the Guava Viacount reagent. This preservation in cell viability is despite the slightly slower growth rates in cells treated with 100 mM sodium butyrate. Interestingly, when measured with Guava Viacount reagent, we observed that the cells treated with 50 mM and 100 mM sodium butyrate exhibited higher viability 57 hours from induction. The final viability for 50 mM and 100 mM was higher from control by 11.41% and 11.81%, respectively. Using the Guava Viacount reagent, we are also able to measure apoptotic cells from the dead cells, thus giving a more accurate representation of apoptotic behavior (*see Figure 12*).

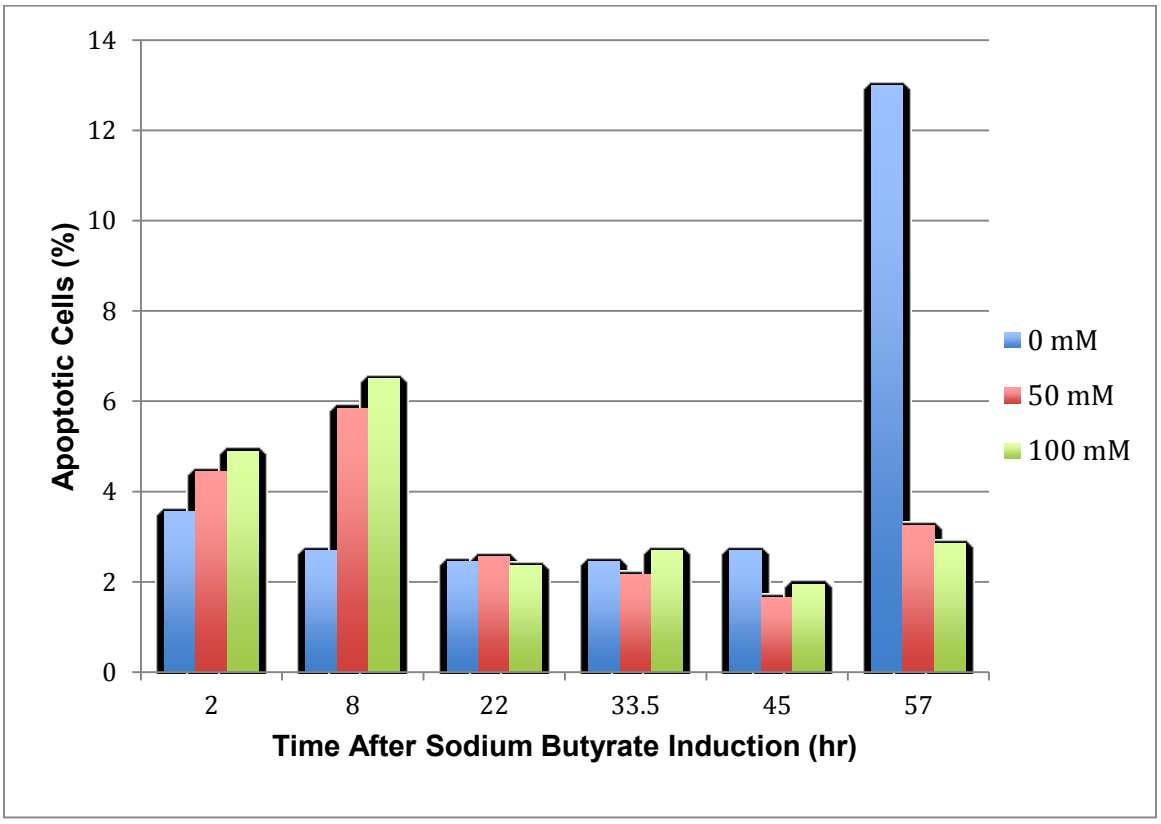

Figure 12: Percent apoptotic of *C. reinhardtii* wall-deficient pRelax cells after sodium butyrate induction.

Using Guava Viacount reagent, we observed that the cells were slightly more apoptotic for several hours immediately after sodium butyrate induction. However, within 22 hours the cells seemed to recover and maintain a low level of apoptotic behavior. The untreated pRelax cells were around 3% apoptotic until about 80 hours after inoculation (or 57 hours after sodium butyrate induction) when the culture became 13% apoptotic. This was in stark contrast to the cultures treated with 50 mM and 100 mM sodium butyrate as their final apoptotic percentage 80 hours after inoculation (or 57 hours after sodium butyrate induction) were 3.25% and 2.85%, respectively. The pRelax cultures treated with 50 mM and 100 mM sodium butyrate were 75% and 78% less apoptotic than untreated pRelax cells, respectively.

As shown previously with the wild-type *C. reinhardtii* wall-deficient cells, the effect of sodium butyrate on cell growth and cell viability can also be observed by looking at the culture with the naked eye (*see Figure 13*).

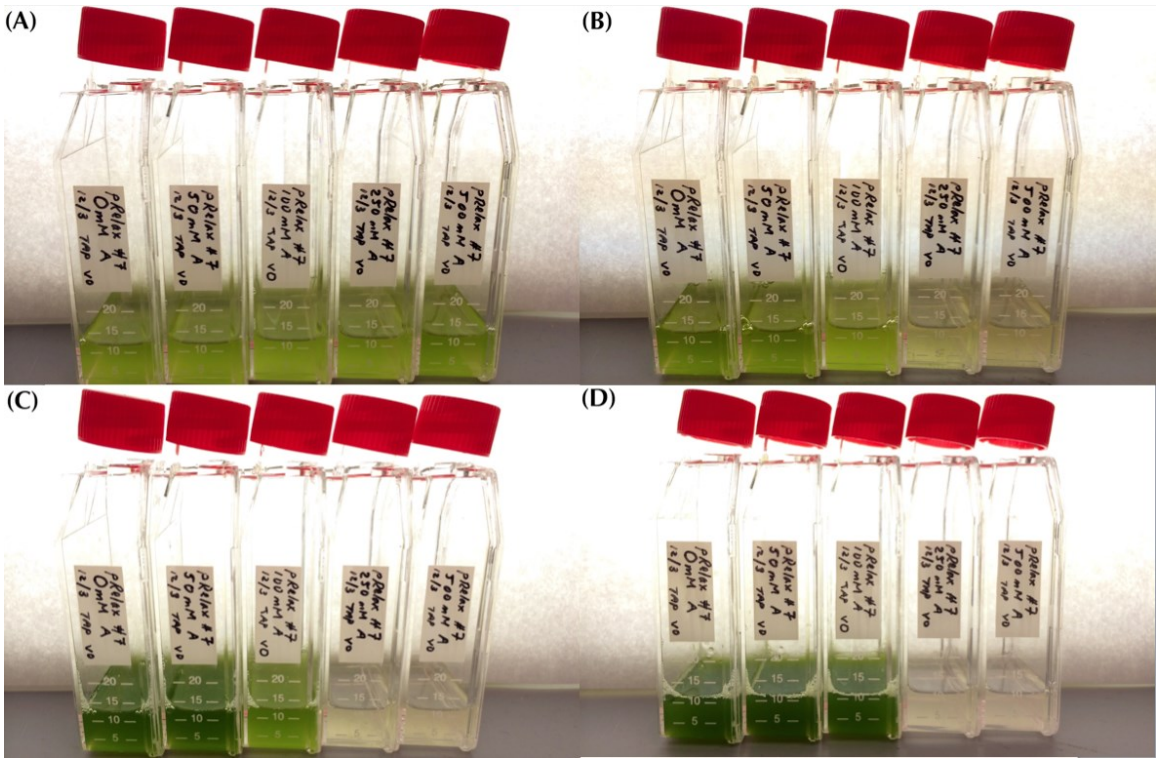

Figure 13: *C. reinhardtii* wall-deficient Venus-Bcl-X_L strain (pRelax) treated with sodium butyrate. From left to right: TAP + 0 mM sodium butyrate, TAP + 50 mM sodium butyrate, TAP + 100 mM sodium butyrate, TAP + 250 mM sodium butyrate, TAP + 500 mM sodium butyrate. (A) 0 hours after sodium butyrate supplementation. (B) 12 hours after sodium butyrate supplementation. (C) 24 hours after sodium butyrate supplementation. (D) 48 hours after sodium butyrate supplementation.

From Figure 13 above, we can observe the progressive growth of the cells treated with 0 mM, 50 mM and 100 mM sodium butyrate. We also see how addition sodium butyrate at concentrations over 250 mM is lethal to the cultures by the immediate blanching of the cultures treated with 250 mM and 500 mM. The slightly slower growth rate of the culture treated with 100 mM can be seen at 12 hours and 24 hours after sodium butyrate induction, along with the convergence of cell densities at 48 hours post induction.

Fluorescent and confocal imaging of sodium butyrate induced pRelax cells

24 hours after sodium butyrate induction, samples were taken for fluorescent imaging to observe any enhanced fluorescence from the Venus-Bcl-x_L fusion protein. At this point, cultures treated with 250 mM and 500 mM sodium butyrate were already dead and thus images are only shown for control, 50 mM, 100 mM treated cells (*see Figure 14*).

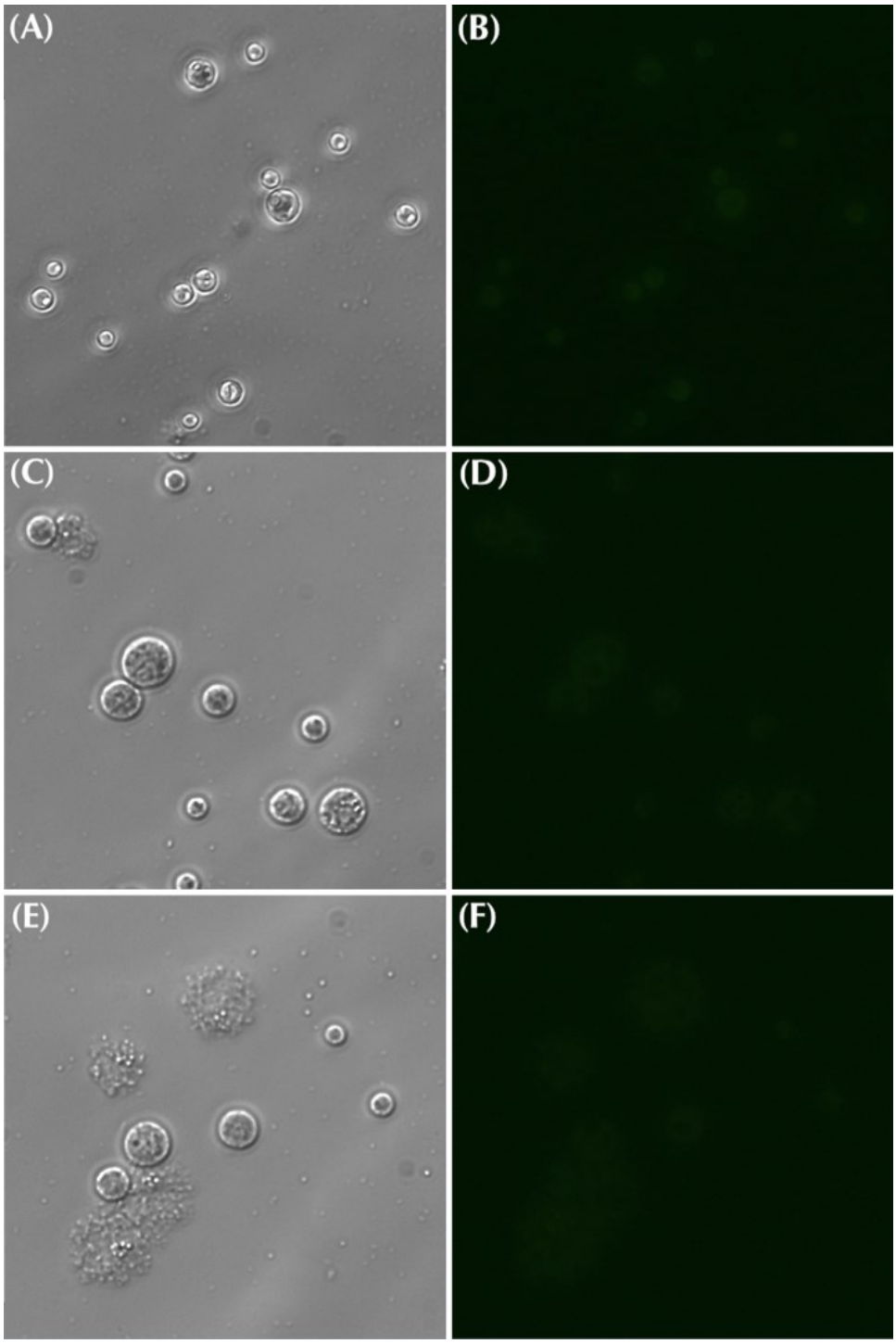

Figure 14: *C. reinhardtii* wall-deficient Venus-Bcl-X_L strain (pRelax) 1 day after sodium butyrate induction. (A) – (B) is TAP + 0 mM sodium butyrate. (C) – (D) is TAP + 50 mM sodium butyrate. (E) – (F) is TAP + 100 mM sodium butyrate. (A), (D), (E) are images taken with Brightfield filter and (B), (D), (F) are images taken with a FITC filter.

As shown in Figure 14 above, the cells treated with 50 mM and 100 mM sodium butyrate exhibit changes in cell morphology as well. The induced cells are larger, with preserved membrane. In the case of the pRelax cells, even untreated cells had very limited mobility or flagellar action (results not shown), so sodium butyrate effect on cell mobility is not easily observed. We applied a FITC filter to excite the Venus protein, to observe any indication of the protein expression. The yellow fluorescent protein reporter, Venus, fused to the Bcl-xL has an excitation wavelength of 515 nm and an emission wavelength 528 nm [75]. As shown in Figure 14 above, the cells do not show high levels of fluorescence. What little fluorescence that is seen is possibly the cell's auto-fluorescence due to the chlorophyll. Chlorophyll has a slight excitation at wavelengths close to 500 nm, which is within the range of the FITC excitation.

Western Blot and protein analysis of recombinant Venus-Bcl-x_L

Due to difficulty in verifying expression of the Venus-Bcl-x_L protein by fluorescence, we proceeded to do protein extraction and analysis by western blotting. The size of Venus is approximately 27 kDa, and the size of Bcl-x_L is about 30 kDa. Therefore, the expected band lengths were approximately 57 kDa for a fusion protein. After protein extraction and western blot, we were unable to observe any bands at the expected locations, while the positive control of a Venus protein was present.

DISCUSSION

Varying concentrations of sodium butyrate were added to suspension cultures of wall-deficient C. *reinhardtii* 45 hours after inoculation. In a preliminary experiment to determine the range of sodium butyrate supplementation, 1 mM, 5 mM, 10 mM, 25 mM, and 50 mM sodium butyrate was added to the cell cultures after 45 hours of growing under normal conditions in TAP media on a rotary shaker in T-25 flasks. Cell counts and microscopy indicated no change in growth behavior and cell morphology at concentrations below 50 mM of sodium butyrate (data not shown). Thus, a subsequent study was done using concentrations of 50 mM, 100 mM, 250 mM, and 500 mM sodium butyrate. The initial range of sodium butyrate concentrations used in the preliminary experiments was based on similar inductions done in transgenic tomato cells. The wild-type wall-deficient C. *reinhardtii* cells were surprisingly tolerant to concentrations of sodium butyrate that would otherwise be lethal for mammalian cells and plant cells that have been so far tested. This may be explained by the fact that simple *n*-butyrate is rapidly metabolized in plant cells during photoautotrophic growth [69].

Sodium butyrate induces changes in cell growth and cell morphology in *C. reinhardtii*

We observed cell growth inhibition of wild-type C. *reinhardtii* cells induced by sodium butyrate at concentrations of 50 mM and 100 mM. These concentrations induced apoptosis in the cells as indicated by decreases in cell viability and also changed the appearance of the cells significantly. Although the exact mechanism behind these observations cannot be concluded through this study, the results are similar to observations

seen in similar studies with mammalian and plant cells. In transgenic tomato cells, treatment with sodium butyrate up-regulated 4 growth-arrest-specific proteins and down regulated two cell division proteins. There is high likelihood that sodium butyrate induces a similar mechanism in mammalian cells and microalgal cells. Similar to many documented results of morphological changes in mammalian cells induced by sodium butyrate, we observed a significant enlargement of the cells. Higher concentrations of sodium butyrate could also lead to higher osmotic pressure, which could be a possible factor in the appearance of swollen cells. The cells may also be going through the cell division or apoptotic stage of their cell cycle, although these would be reflected in the cell growth curves or apoptosis graphs.

Expression and function of recombinant Venus-Bcl-x_L protein

The treatment of the pRelax strain with sodium butyrate produced interesting results. There was significantly less inhibition of cell growth compared to the wild-type cells at the same concentration of sodium butyrate. Despite the observed tolerance to the apoptotic inducing effects of sodium butyrate, the pRelax cells did not have noteworthy levels of fluorescence or protein. PCR also confirmed the presence of the vector sequence in the nuclear genome. Some explanations for the lack of observed fluorescence is the extremely low expression of the protein along with the localization of the protein to the mitochondria. The mitochondria is a small organelle located near the nucleus, so with observation at 20x using a fluorescent microscope would make it difficult to see clear fluorescence to begin with. The most probable explanation for the absence of positive

bands from the western blot is the low expression of the target recombinant protein along with the relatively low quantities of cells harvested. Although the density was at about 12 x 10^6 cells/mL, only around 10 mL were cultured. Since the expected expression level of Venus-Bcl-xL is low, the culture should be scaled-up for a subsequent study with supplementation at the same range of sodium butyrate concentrations, and then harvested for protein extraction.

Another possibility for lack of observed expression is the limitation of the protein extraction method. Although we utilized a sonication method with cell lysis buffer and protease inhibitors, it is possible that the protein was either degraded by the sonication, or never fully extracted due to its localization to the mitochondria. In this event, the cell lysate should also be analyzed for the possible presence of Venus-Bcl-x_L protein.

Although the expression of the protein could not be verified with fluorescence or western blotting, the results of tolerance and resistance to apoptosis shown in cell growth curves and viability charts indicate the presence and functionality of the Venus-Bcl-x_L protein. While the level of expression may be low, there seems to be an enhancement of anti-apoptotic behavior in pRelax cells treated with 50 mM and 100 mM sodium butyrate. It can be hypothesized that this is in fact due to an up-regulation of transgene expression induced by sodium butyrate, although exact conclusions cannot be made without further analysis.

CONCLUSION

For decades, the effect of sodium butyrate has been studied in mammalian cells and plant cells. There has been particular interest in the transgene expression enhancing effects of sodium butyrate in these systems. Surprisingly, almost no literature or documentation is available on the application of sodium butyrate in microalgae systems. This study explored the effects of exposing microalgae *C. reinhardtii* to sodium butyrate in varying concentrations ranging from 0 mM to 500 mM and observing the possible changes in cell growth, cell morphology and transgene expression.

Green microalgae *C. reinhardtii* seems inherently tolerant to the expected effects of sodium butyrate, and thus changes in cell growth and morphology were observable at concentrations above 50 mM, over ten times the lethal concentration for most tested mammalian cells. However, at concentrations of 50 mM and 100 mM sodium butyrate, we observed inhibition of cell growth along with induction of apoptosis. At these concentrations the cells appeared larger and rounder, with seemingly enlarged nuclei. Concentrations above 250 mM were deadly to the cells and quickly induced apoptosis as observed by cell growth curves, viability measurements, and microscopy.

A transgenic cell line of *C. reinhardtii* expressing a mammalian anti-apoptotic Venus-Bcl-x_L fusion protein was also treated with a range of sodium butyrate concentrations. These cells were significantly tolerant to the sodium butyrate stress and exhibited resistance to apoptosis compared to the wild-type strain of *C. reinhardtii*. Even within the same cell-line,

pRelax cells treated with 50 mM and 100 mM sodium butyrate were 75% and 78% less apoptotic than untreated pRelax cells, respectively. Although protein expression was not confirmed by western blot or fluorescence microscopy, these results suggest a possible induction of enhanced transgene expression.

The potential for microalgae as a standard molecular farming platform is promising due to its high growth rate and relatively scalability. The versatility of the nuclear genome in performing post-transcriptional, post-translational modifications, and post-translational targeting to specific intracellular organelles make nuclear expression from microalgae a powerful potential alternative to current expression systems. Unfortunately, due to the high levels of transgene silencing frequently experienced in the nuclear genome, microalgae is still far from realizing its full potential as a revolutionary recombinant protein expression platform.

Much of the efforts in tackling low expression of recombinant proteins from the nucleus are focused on optimizing design at the genetic level with promoters, codon optimization, and plasmid designs. This study outlines a potential avenue focused on the downstream side of process design through sodium butyrate supplementation of the suspended microalgal cultures. Sodium butyrate has been shown to induce apoptosis in mammalian cell lines and inhibit cell growth in various mammalian cells and plant cells. In this study, these changes were similarly observed in microalgae upon sodium butyrate induction at concentrations of 50 mM and 100 mM. Induced apoptosis and inhibition of cell growth was reversible over time and the cells were able to recover after 24 – 48 hours. Along with inducing apoptosis and inhibition of cell growth, sodium butyrate is known to enhance transgene expression in various mammalian cell lines and plant cell lines. Although similar

results cannot be readily concluded from this study, we observe the enhanced functionality of an anti-apoptotic recombinant Venus-Bcl-x_L fusion protein in a transgenic strain of microalgae *C. reinhardtii* treated with 50 mM and 100 mM sodium butyrate. The use of an expressed Bcl-x_L protein to resist the induction of apoptosis of sodium butyrate treated cells has interesting implications for a powerful combination system that integrates the powerful transgene enhancing capabilities of sodium butyrate supplementation with the anti-apoptotic function of Bcl-x_L to negate the side-effects of sodium butyrate exposure. The model system would have the target protein of interest co-expressed with a Bcl-x_L protein. Sodium butyrate supplementation would then, in concept, induce higher expression of both proteins. Although it is preliminary, this study shows promising signs of the applicability of using a sodium butyrate, and the coupled effect of an anti-apoptotic Bcl-x_L protein, to enhance the protein yield in molecular farming.

REFERENCES

[1] A. Villaverde, *et al.* Microbial factories for recombinant pharmaceuticals. *Microbial Cell Factorie;s* **8:**17 (2009).

[2] A. Villaverde, *et al.* Unconventional microbial systems for the cost-efficient production of high-quality protein therapeutics. *Biotechnology Advances* 31 140-153 (2013).

[3] SS Farid. Process economics of industrial monoclonal antibody manufacture. *J Chromatogr B Analyt Technol Biomed Life Sci;* 848(1):8-18 (2007).

[4] SP Mayfield, *et al.* Optimization of Recombinant Protein Expression in the Chloroplasts of Green Algae

[5] Tara L. Walker, *et al.* Microalgae as bioreactors.

[6] F Baneyx, M Mujacic. Recombinant protein folding and misfolding in Escherichia coli. *Nat Biotechnol*;22(11):1399–408 (2004).

[7] R Fischer, YC Liao, K Hoffmann, S Schillberg, N Emans Molecular farming of recombinant antibodies in plants. *Biol Chem* 380:825–839 (1999).

[8] N Jenkins. Modifications of therapeutic proteins: challenges and prospects**.** *Cytotechnology*, **53:**121-125 (2007).

[9] V Gomord, *et al.* Plant-specific glycosylation patterns in the context of therapeutic protein production. *Plant Biotechnology Journal*; 8, pp. 564–587 (2010)

[10] Florian M Wurm. Production of recombinant protein therapeutics in cultivated mammalian cells. *Nature Biotechnology* Volume 22, Number 11, (2004).

[11] MR Scott, R Will, J Ironside, HO Nguyen, P Tremblay, SJ DeArmond, SB Prusiner. Compelling transgenic evidence for transmission of bovine spongiform encephalopathy prions to humans. *Proc Natl Acad Sc;* 96:15137–15142 (1999).

[12] C Mohan, YG Kim, J Koo, GM Lee. Assessment of cell engineering strategies for improved therapeutic protein production in CHO cells. *Biotechnol J*, **3:**624-630 (2008).

[13] J.L. Corchero, *et al.* Unconventional microbial systems for the cost-efficient production of high-quality protein therapeutics. *Biotechnology Advances* 31 140–153 (2013).

[14] R Passwater, *et al.* Algae: the next generation of superfoods. *Exp Op Health J* 1:2-10 (1997).

[15] M Hippler, K Redding, JD Rochaix. Chlamydomonas genetics, a tool for the study of bioenergetic pathways. *Biochim. Biophys. Acta,* 1367, 1–62 (1998).

[16] EH Harris. Chlamydomonas as a model organism. *Annu. Rev. Plant Physiol. Plant Mol. Biol.* 52, 363–406 (2001).

[17] LB Pedersen, S Geimer, JL Rosenbaum. Dissecting the molecular mechanisms of intraflagellar transport in Chlamydomonas. *Curr. Biol.* 16, 450–459 (2006).

[18] M Schmidt, G Gebner, M Luff, *et al.* Proteomic analysis of the eyespot of Chlamydomonas reinhardtii provides novel insights into its components and tactic movements. *Plant Cell*, 18, 1908–1930 (2006).

[19] Stephen Mayfield, *et al.* Micro-algae come of age as a platform for recombinant protein production. *Biotechnology Letter* 32:1373-1383 (2010).

[20] SS Merchant, SE Prochnik, O Vallon, *et al.* The Chlamydomonas genome reveals the evolution of key animal and plant functions. *Science* 318, 245–251 (2007).

[21] J Neupert, D Karcher, R Bock. Generation of *Chlamydomonas* strains that efficiently express nuclear transgenes. *The Plant Journal* **57**, 1140-1150 (2009).

[22] L Bogorad. Engineering chloroplasts: An alternative site for foreign genes, reactions and products. *Trends Biotechnoi*; 18:257-263 (2000).

[23] Maul JE, Lilly JW, Cui L, dePamphilis CW, Miller W, Harris EH, Stern DB The *Chlamydomonas reinhardtii* plastid chromosome: islands of genes in a sea of repeats. *Plant Cell* 14:2659-2679 (2002).

[24] Mayfield SP, Franklin SE, Lerner RA. Expression and assembly of a fully active antibody in algae. *Proc Natl Acad Sci*; 100(2):438–42 (2003).

[25] Zhang Z, Potvin G. Strategies for high-level recombinant protein expression in transgenic microalgae: A review. *Biotechnology Advances* 28: 910-918 (2010).

[26] Maiiga P. Plastid transformation in higher plants. *Annu Rev Plant Biol*; 55:289-313 (2004).

[27] Tam LW, Lefebvre PA. Cloning of flagellar genes in *Chlamydomonas reinhardtii* by DNA insertional mutagenesis. *Genetics* 135:375-384 (1993).

[28] Goldschmidt-Clermont M Transgenic expression of aminoglycoside adenine trasnferase in the chloroplast: a selectable marker for site-directed transformation of *Chlamydomonas*. *Nucleic Acids Res* 19:4083-4089 (1991).

[29] Surzycki R, Greenham K, Kitayama K, Dibal F, Wagner R, Rochaix JD, et al. Factors effecting expression of vaccines in microalgae. *Biol*;37:133–8 (2009).

[30] Mayfield S, *et al.* Production of therapeutic proteins in algae, analysis of expression of seven human proteins in the chloroplast of Chlamydomonas reinhardtii. *Plant Biotechnology Journal* 8, pp. 719–733 (2010).

[31] Rosales-Mendoza, *et al. Chlamydomonas reinhardtii* as a viable platform for the production of recombinant proteins: current status and perspectives. *Plant Cell Rep 31:479 – 494 (2012).*

[32] Cadoret JP, et al. Microalgae, Functional Genomics and Biotechnology

[33] Kurland C, Gallant J. Errors of heterologous protein expression. *Curr Opin Biotechnol*; 7(5):489-93 (1996).

[34] Jarvis, E.E. et al. DNA nucleoside composition and methylation of several species of microalgae. *J. Phycol.* 28, 356 – 362 (1992).

[35] Nakamura Y, Gojobori T, Ikemura T. Codon usage tabulated from the international DNA sequence databases. *Nucleic Acids Res* 27:292–298 (1999)

[36] Franklin S, Ngo B, Efuet E, Mayfield SP Development of a GFP reporter gene for Chlamydomonas reinhardtii chloroplast. *Plant J* 30:733–744 (2002).

[37] Hoffmann XK, Beck CF. Mating-induced shedding of cell walls, removal of walls from vegetative cells and osmotic stress induce presumed cell wall genes in Chlamydomonas. *Plant Physiol*;139:999-1014 (2005).

[38] Kindle KL. High frequency nuclear transformation of Chlamydomonas reinhardtii. *Proc Natl Acad Sci*;87:1228–32 (1990).

[39] Kindle KL, Richards KL, Stern DB. Engineering the chloroplast genome: techniques and capabilities for chloroplast transformation in Chlamydomonas reinhardtii. *Proc Natl Acad Sci*;88:1721–5 (1990).

[40] Cohen, A., Yohn, C.B., Bruick, R.K. and Mayfield, S.P. Translational regulation of chloroplast gene expression in Chlamydomonas reinhardtii. *Methods Enzymol.* 297, 192–208 (1998).

[41] Boynton JE, Gillham NW. Chloroplast transformation in Chlamydomonas. *Methods. Enzymol*;217:510–36 (1993).

[42] Shimogawara K, Fujiwara S, Grossman A, Usuda H. High-efficiency transformation of Chlamydomonas reinhardtii by electroporation. *Genetics*;148:1821–8 (1998).

[43] Brown LE, Sprecher SL, Keller LR. Introduction of exogenous DNA into Chlamydomonas reinhardtii by electroporation. *Mol Cell Biol*;11:2328–32 (1991).

[44] Azencott HR, Peter GF, Prausnitz MR. Influence of the cell wall on intracellular delivery to algal cells by electroporation and sonication. *Ultrasound Med Biol*;33: 1805–17 (2007).

[45] Kumar SV, Misquitta RW, Reddy VS, Rao BJ, Rajam MV. Genetic transformation of the green alga—Chlamydomonas reinhardtii by Agrobacterium tumefaciens. *Plant Sci* 166:731–8 (2004).

[46] J. N. Rosenberg, Overcoming obstacles to biofuel production: species selection & genetic engineering of stress tolerance. *Transformation*. October, (2009).

[47] T. Nagai, K. Ibata, E. S. Park, M. Kubota, K. Mikoshiba, and A. Miyawaki, "A variant of yellow fluorescent protein with fast and efficient maturation for cell-biological applications.," *Nature biotechnology*, vol. 20, no. 1, pp. 87-90 (2002).

[48] L. H. Boise et al., Bcl-X, a Bcl-2-Related Gene That Functions As a Dominant Regulator of Apoptotic Cell Death. *Cell*, vol. 74, no. 4, pp. 597-608 (1993).

[49] P. Xu, S. J. Rogers, and M. J. Roossinck. Expression of antiapoptotic genes bcl-xL and ced-9 in tomato enhances tolerance to viral-induced necrosis and abiotic stress. *Proceedings of the National Academy of Sciences of the United States of America*, vol. 101, no. 44, pp. 15805-10 (2004).

[50] M Schroda, *et al.* The HSP70A promoter as a tool for the improved expression of transgenes in *Chlamydomonas*. *Plant J*, 21:121-131 (2000).

[51] M. Schroda, *et al.* Sequence elements within an *HSP70* promoter counteract transcriptional transgene silencing in *Chlamydomonas*. *The Plant Journal* **31**(4), 445-455 (2002).

[52] DP Palemermo, *et al.* Production of analytical quantities of recombinant proteins in Chinese hamster ovary cells using sodium butyrate to elevate gene expression. *Journal of Biotechnology,* 19 35-58 (1991).

[53] C Rius, C Cabanas, P Aller. The induction of vimentin gene expression by sodium butyrate in human promonocytic leukemia U937 cells. *Experimental Cell Research* **188,** 129-134 (1990).

[54] KN Prasa, PK Sinha. Effect of sodium butyrate on mammalian cells in culture: a review. *In Vitro*. Vol 12, No. 2. (1976).

[55] Wright JA. Morphology and growth rate changes in Chinese hamster cells cultured in presence of sodium butyrate. *Exptl Cell Res* 78 456-460 (1973).

[56] Pederson TJ, Minocha SC. Effect of n-sodium butyrate on cell division in Jerusalem artichoke (*Helianthus tuberosus* L.) tuber explants cultured *in vitro. J. Plant Physiol.* **132**: 623-630 (1988).

[57] IS Chung, *et al.* Improved production of recombinant rotavirus VP6 in sodium butyrate-supplemented suspension cultures of transgenic tomato (*Lycopersicon esculentum* Mill.) cells. *Biotechnology Letters* **23:** 1061-1066 (2001).

[58] CM Gorman, *et al.* Expression of recombinant plasmids in mammalian cells is enhanced by sodium butyrate. *Nucleic Acids Res.* 11, 7631-7648 (1983).

[59] T Kooistra, *et al.* Stimulation of tissue-type plasminogen activator gene expression by sodium butyrate and trichostatin A in human endothelial cells involves histone acetylation. *Biochem J.* **310**, 171-176 (1995).

[60] JH Waterborg, *et al.* Dynamic histone acetylation in alfalfa cells. Butyrate ingerference with acetate labeling. *Biochimica et Biophysica Acta,* 1049, 324-330 (1990).

[61] James R. Davie, *et al.* Role of covalent modifications of histones in regulating gene expression. Gene 240 1-12 (1999).

[62] K Luger, *et al.* Crystal structure of the nucleosome core particle at 2.8 A resolution. *Nature* 389, 251-260 (1997).

[63] M Garcia-Ramirez, *et al.* Modulation of chromatin folding by histone acetylation. *J. Biol. Chem.* 270, 17923-17928 (1995).

[64] H Walia, *et al.* Histone acetylation is required to maintain the unfolded nucleosome structure associated with transcribing DNA. *J. Biol. Chem.* 273, 14516-24522.

[65] Allfrey, V. G. in Chromatin and Chromosome Structure (Li, H. J., and Eckhardt, R. A., eds) pp. 167–191, Academic Press, New York (1977).

[66] Matthews, H. R., and Waterborg, J. H. in *The Enzymology of Post- translational Modification of Proteins* (Freedman, R. B., and Hawkins, H. C., eds) Vol. 2, pp. 125–285, Academic Press, London (1985).

[67] Davie, J. R., and Hendzel, M. J. *J. Cell. Biochem*. 55, 98–105 (1994).

[68] Grunstein, M. *Nature* 389, 349–352 (1997).

[69] Waterborg, Jakob H. Dynamics of Histone Acetylation in *Chlamydomonas reinhardtii*. *The Journal of Biological Chemistry*. Vol. 273, No. 42, Issue of October 16, pp. 27602-27609 (1998).

[70] A. L. Edinger and C. B. Thompson. Death by design: apoptosis, necrosis and autophagy. *Current opinion in cell biology*, vol. 16, no. 6, pp. 663-9, (2004).

[71] I. V. Shemarova. Signaling mechanisms of apoptosis-like programmed cell death in unicellular eukaryotes. *Comparative biochemistry and physiology. Part B, Biochemistry & molecular biology*, vol. 155, no. 4, pp. 341-53 (2010).

[72] E. H. Cheng et al., BCL-2, BCL-X(L) sequester BH3 domain-only molecules preventing BAX- and BAK-mediated mitochondrial apoptosis. *Molecular cell*, vol. 8, no. 3, pp. 705-11 (2001).

[73] L. H. Boise et al. Bcl-X, a Bcl-2-Related Gene That Functions As a Dominant Regulator of Apoptotic Cell Death. *Cell*, vol. 74, no. 4, pp. 597-608, (1993).

[74] T. Kuwana et al. Bid, Bax, and lipids cooperate to form supramolecular openings in the outer mitochondrial membrane. *Cell*, vol. 111, no. 3, pp. 331-42, (2002).

[75] T. Nagai, K. Ibata, E. S. Park, M. Kubota, K. Mikoshiba, and A. Miyawaki. A variant of yellow fluorescent protein with fast and efficient maturation for cell-biological applications. *Nature biotechnology*, vol. 20, no. 1, pp. 87-90, (2002).

APPENDIX

Sodium Butyrate Induction of Wild-type *C. reinhardtii:*

		TOTAL CELLS/mL									
		Cells/mL									
		0mM_1	0mM_2	50mM_1	50mM_2	100mM_1	100mM_2	250mM_1	250mM_2	500mM_1	500mM_2
Time (hours)	0	0.25	0.25	0.25	0.25	0.25	0.25	0.25	0.25	0.25	0.25
	19.5	0.5341 35982	0.4185 40532	0.3989 07941	0.3914 14623	0.3893 71589	0.3345 93394	0.5587 52525	0.5436 75313	0.5122 65843	0.4324 13781
	30	0.3041 1899	0.3754 87866	0.4804 95021	0.3576 73227	0.4719 61998	0.4275 6463	0.6351 77895	0.4746 2235	0.5215 37105	0.4847 93175
	42	0.8100 07945	1.5827 61005	1.4461 30805	0.7798 5016	0.6852 40671	0.6731 75292	1.0399 38371	1.0810 48206	1.2338 32935	1.1297 74918
	46	1.2339 42274	1.0271 76627	1.3551 96802	1.3835 23995	1.6751 30813	1.9342 06994	2.0837 38221	2.4255 44192	2.7470 82665	2.1380 50217
	54	1.8027 76389	1.1354 98489	1.4792 68721	1.3582 19307	1.6809 00468	1.6462 53716	2.4972 11908	2.1897 1733	0.5231 7928	0.4075 59813
	66.5	5.8904 84596	2.2943 78217	2.6990 92768	2.1769 59078	1.7834 31868	1.2110 14733	1.3239 16793	0.5966 5123	0	0
	78	6.8165 32633	6.5095 62827	10.285 46952	8.4373 48365	2.9705 33392	2.4061 95917	0.0876 56667	0.0895 33333	0	0
	90	13.315 50946	10.482 22041	12.329 30986	10.045 23386	5.1944 30068	3.6840 08753	0	0	0	0

		Viability									
		0mM_1	0mM_2	50mM_1	50mM_2	100mM_1	100mM_2	250mM_1	250mM_2	500mM_1	500mM_2
Time (hours)	0	100	100	100	100	100	100	100	100	100	100
	19.5	99.2	99.2	99.033 33333	99.1	98.766 66667	99	99.266 66667	99.233 33333	99.366 66667	99.333 33333
	30	99.3	98.966 66667	99.533 33333	99.533 33333	99.1	99.133 33333	99.333 33333	98.966 66667	98.966 66667	98.8
	42	98.966 66667	98.766 66667	99	98.166 66667	98.333 33333	98.166 66667	93.066 66667	92.8	94.033 33333	91.666 66667
	46	98.9	98.633 33333	98.733 33333	98.666 66667	99.133 33333	98.8	93.266 66667	91.6	47.866 66667	45.533 33333
	54	96.8	95.4	95.266 66667	93.7	96.566 66667	94.866 66667	39.366 66667	14.933 33333	0	0
	66.5	98.066 66667	96.8	94.266 66667	91.966 66667	93.766 66667	90.266 66667	0.6333 33333	1.67	0	0
	78	99	98.333 33333	97.533 33333	96.566 66667	91.7	89.8	0.1	0.0333 33333	0	0
	90	98.733 33333	98.933 33333	97.433 33333	96.733 33333	94.766 66667	93.066 66667	0	0	0	0

		Standard Error (Total Cells)									
		0mM_1	0mM_2	50mM_1	50mM_2	100mM_1	100mM_2	250mM_1	250mM_2	500mM_1	500mM_2
Time (hours)	0	0	0	0	0	0	0	0	0	0	0
	19.5	0.0193 1794	0.0090 72713	0.0196 48181	0.0083 72658	0.0093 38507	0.0096 42094	0.0407 1519	0.0473 56767	0.0242 95535	0.0091 17503
	30	0.0175 01827	0.0410 2455	0.1211 82672	0.0515 55265	0.0734 03126	0.1143 24966	0.0455 99232	0.0518 71558	0.0260 54068	0.0824 61096
	42	0.0255 40999	0.0404 22666	0.0453 88838	0.0792 67719	0.0953 2413	0.0629 21854	0.1267 47752	0.0673 07217	0.0808 141	0.0391 54214
	46	0.0384 6228	0.0413 70885	0.0395 76768	0.0563 4588	0.0738 9469	0.0871 11618	0.0439 57	0.1212 51386	0.0843 93245	0.0663 36269
	54	0.0204 33221	0.0257 87834	0.0858 00821	0.1063 22647	0.0237 00563	0.0312 92951	0.0432 88075	0.0564 90316	0.0212 30828	0.0109 63313
	66.5	1.1094 35761	0.3391 89396	0.2237 27333	0.0947 3403	0.2619 44152	0.3073 87389	0.0262 82436	0.0165 2355	0	0
	78	1.4355 50929	0.5740 43911	0.3703 75518	0.4446 03606	0.1042 35272	0.0507 54438	0.0876 56667	0.0895 33333	0	0
	90	1.8211 70948	1.0212 61763	0.4824 19415	0.3746 73918	0.2048 36362	0.1921 85642	0	0	0	0

		Standard Error (Viability)									
		0mM_1	0mM_2	50mM_1	50mM_2	100mM_1	100mM_2	250mM_1	250mM_2	500mM_1	500mM_2
Time (hours)	0	0	0	0	0	0	0	0	0	0	0
	19.5	0.1732 05081	0.1154 70054	0.0333 33333	0.1154 70054	0.1201 85043	0.0577 35027	0.1452 96631	0.1763 83421	0.0881 9171	0.0666 66667
	30	0.1527 52523	0.1201 85043	0.1201 85043	0.0881 9171	0.1	0.1855 92145	0.0333 33333	0.2962 73147	0.0333 33333	0.2516 61148
	42	0.1763 83421	0.2185 81284	0.1154 70054	0.0881 9171	0.3756 47589	0.1201 85043	0.9562 65886	0.1154 70054	0.5238 74455	0.1855 92145
	46	0.2081 666	0.2333 33333	0.2333 33333	0.2027 58751	0.1452 96631	0.1732 05081	0.2848 00125	0.6658 32812	0.5238 74455	0.6691 61997
	54	0.5686 2407	0.0577 35027	0.5238 74455	0.8082 90377	0.5696 0025	0.4702 24533	0.3282 9526	0.5456 90185	0	0
	66.5	0.2027 58751	0.6928 20323	0.3844 18753	0.5783 11719	0.5696 0025	1.5213 29828	0.1201 85043	0.1709 77581	0	0
	78	0.1527 52523	0.3480 10217	0.2728 45092	0.1452 96631	0.7505 5535	0.2886 75135	0.1	0.0333 33333	0	0
	90	0.2027 58751	0.0666 66667	0.2905 93263	0.4630 81466	0.5811 86526	0.4371 62568	0	0	0	0

Sodium Butyrate Induction of pRelax:

	TOTAL CELLS/mL				
	Cells/mL				
	0mM	50mM	100mM	250mM	500mM
0	0.5	0.5	0.5	0.5	0.5
21	1.376417068	1.416597624	1.045854585	1.052582223	1.924819092
24.5	1.501912503	1.11727886	0.827692677	0.592665881	0.146044403
30.5	2.258380863	1.391900577	0.783402326	0.173276148	0.004568027
44.5	5.023428777	5.101885395	3.183771287	0	0
56	9.864717	9.395252527	4.930937959	0	0
67.5	11.45165777	13.76014581	10.17741211	0	0
79.5	11.19594043	14.08352002	10.85727191	0	0

Time (hours)

	VIABLE CELLS/mL				
	Cells/mL				
	0mM	50mM	100mM	250mM	500mM
0	0.5	0.5	0.5	0.5	0.5
21	1.36503896	1.39872821	1.02845067	1.040920817	1.898534543
24.5	1.477646627	1.099361147	0.814113503	0.433997633	0.001709057
30.5	2.2243525	1.374727337	0.767165417	0.046596847	0.00006715
44.5	4.921574	5.055948	3.15401625	0	0
56	9.747512667	9.305599	4.883101	0	0
67.5	11.26342833	13.64458933	10.13233833	0	0
79.5	10.96120967	13.89254367	10.74133933	0	0

Time (hours)

	Standard Error (Total Cells)				
	0mM	50mM	100mM	250mM	500mM
0	0	0	0	0	0
21	0.06983315	0.100568029	0.054384683	0.046201862	0.071236527
24.5	0.04163329	0.071682545	0.015197694	0.015914345	0.00162459
30.5	0.039566757	0.038661228	0.011744203	0.005121146	0.004568027
44.5	0.124263857	0.153517576	0.061045913	0	0
56	0.299822794	0.548260386	0.114020435	0	0
67.5	0.457935328	0.329683759	0.594306219	0	0
79.5	0.120278508	0.825597259	0.299011622	0	0

Time (hours)

	Standard Error (Viability)					
		0mM	50mM	100mM	250mM	500mM
Time (hours)	0	0	0	0	0	0
	21	0.176383421	0.145296631	0.504424865	0.290593263	0.32829526
	24.5	0.435889894	0.1	0.218581284	0.721880261	0.218581284
	30.5	0.2081666	0.260341656	0.260341656	0.721880261	0.49
	44.5	0.272845092	0.152752523	0.033333333	0	0
	56	0.346410162	0.185592145	0.218581284	0	0
	67.5	0.145296631	0.145296631	0.218581284	0	0
	79.5	0.251661148	0.120185043	0.033333333	0	0

	TOTAL CELLS/mL (GUAVA)					
		Cells/mL				
		0mM	50mM	100mM	250mM	500mM
Time (hours)	0	500000	500000	500000	500000	500000
	21	1376417.068	1416597.624	1045854.585	1052582.223	1924819.092
	24.5	1165300.421	955438.9414	748240.1482	675815.6534	510393.3333
	30.5	1937180.642	1295515.982	699299.7585	237458.8499	30283.33333
	44.5	4603020.187	5124294.584	2819384.615	0	0
	56	9153378.996	10197592.82	4232535.501	0	0
	67.5	13214317.24	12055832.48	7663538.079	0	0
	79.5	12274857.42	12320819.37	12234885.26	0	0

	VIABILITY (GUAVA)					
		0mM	50mM	100mM	250mM	500mM
Time (hours)	0	100	100	100	100	100
	21	99.16666667	98.73333333	98.33333333	98.86666667	98.63333333
	24.5	95.55	95.45	94.7	56.7	0.9
	30.5	96.6	93.8	93	27.75	0.5
	44.5	97.5	97.1	97.5	3.3	0.2
	56	97.55	97.8	97.15	0	0
	67.5	97.1	98.3	97.95	0	0
	79.5	86.8	96.7	97.05	0	0

	PERCENT APOPTOTIC (GUAVA)					
		0mM	50mM	100mM	250mM	500mM
Time (hours)	0					
	21					
	2	3.55	4.45	4.9	26	28.5
	8	2.7	5.85	6.5	30.9	2.5
	22	2.45	2.55	2.35	59.9	2.4
	33.5	2.45	2.15	2.7		
	45	2.7	1.65	1.95		
	57	13	3.25	2.85		

	Standard Error (Total Cells)					
		0mM	50mM	100mM	250mM	500mM
Time (hours)	0	0	0	0	0	0
	21	0.06983315	0.100568029	0.054384683	0.046201862	0.071236527
	24.5	0.038164281	0.000815803	0.011957735	0.022245411	0.023312792
	30.5	0.067330676	0.016017735	0.034811485	0.01039736	0.024726238
	44.5	0.047328991	0.178601923	0.064527515	0	0
	56	0.418575205	0.464268317	0.078550426	0	0
	67.5	0.65545851	0.830919968	0.000298263	0	0
	79.5	0.537049485	0.141797758	0.667395614	0	0

	Standard Error (Viability)					
		0mM	50mM	100mM	250mM	500mM
Time (hours)	0	0	0	0	0	0
	21	0.21602469	0.145296631	0.504424865	0.290593263	0.32829526
	24.5	0.15	0.040824829	0.163299316	0.816496581	0
	30.5	0.5	0.816496581	0.163299316	0.816496581	0.163299316
	44.5	0.163299316	0.40824829	0	0.081649658	0.081649658
	56	0.530722778	0.163299316	0.204124145	0	0
	67.5	0.163299316	0.163299316	0.122474487	0	0
	79.5	0.40824829	0.40824829	0.44907312	0	0